et al., 1999; Jialal et al., 2001; Kwak et al., 2001). These lipid- and non-lipid-related effects are considered to be protective against cardiovascular diseases (Plenge et al., 2002; Wassmann et al., 2003).

Recently, many extensive epidemiological studies have demonstrated that AMD shares a number of overlapping risk factors with atherosclerosis, including age, cigarette smoking, hypertension, obesity, and increased dietary fat intake (Mitchell et al., 1995; Klaver et al., 2001; McCarty et al., 2001; Mitchell et al., 2002). Considering their well-established effectiveness in cardiovascular disease, statins may also be effective in the management of AMD. In recent years, a small cross-sectional survey suggested that statins exert a protective effect in AMD (Hall et al., 2001). However, subsequent studies have produced inconsistent results (McCarty et al., 2001; McGwin et al., 2003; Klein et al., 2003; Wilson et al., 2004; McGwin et al., 2006).

In this study, we evaluated the effect of the administration of pitavastatin (so-called vascular statin), which has a high affinity for vascular endothelium, on experimental CNV created by laser-induced rupture of Bruch's membrane, which stimulates preexisting capillaries to proliferate into new capillary networks, in rats. The murine model of experimental CNV was used because rats are resistant to the hypocholesterolemic effect of statins.

2. Materials and methods

2.1. Experimental CNV model in rats

Six-week-old male Brown Norway (BN) rats (Seac Yoshitomi, Fukuoka, Japan) weighing 120–160 g were used. The animals were handled in accordance with institutional guidelines and the ARVO Statement for the Use of Animals in Ophthalmic and Vision Research. The BN rats were anesthetized by intramuscular injection of a 1 mL/kg mixture (1:1) of ketamine hydrochloride (Ketalar; Sankyo, Tokyo, Japan) and xylazine hydrochloride (Celactal; Bayer, Tokyo, Japan), and their pupils were dilated with tropicamide (0.5% Mydrin M; Santen Pharmaceutical, Osaka, Japan). Experimental CNV was created as described previously (Takehana et al., 1999). Briefly, four laser photocoagulations were applied to each eye between the major retinal vessels around the optic disk under the following conditions: power 150 mW, wavelength 521 nm, duration 100 ms and spot size 100 μm. Bruch's membrane was breached, as evidenced clinically by central bubble formation, without intraretinal or choroidal hemorrhage.

2.2. Drug administration

The total 38 BN rats were divided into two groups: pitavastatin-treated ($n = 19$) and vehicle-treated ($n = 19$). Pitavastatin (Livalo, previously known as NK-104) was kindly provided by Kowa (Tokyo, Japan). It was dissolved in 0.5% carboxymethylcellulose (CMC) sodium salt (Wako, Osaka, Japan) and administered at a dose of 1 mg kg^{-1} day^{-1} (pitavastatin-treated rats). Control rats (vehicle-treated rats) received 0.5% CMC vehicle. Oral gavage was performed with a 20-gauge blunt feeding needle for 1 day prior to the laser induction of CNV and continued daily until the rats were killed and evaluated.

2.3. Fluorescein angiography

At day 14 after laser induction of CNV, the laser lesions were studied by fluorescein angiography to evaluate CNV development and its activity. Each rat was injected with 0.5 ml of 10% fluorescein sodium (Fluorescite; Alcon, Tokyo, Japan) intraperitoneally, and fundus angiogram photographs were taken at early and late phases using a scanning laser ophthalmoscope (SLO101; Rodenstock, Germany). The formation of CNV was evaluated according to the size and the presence or absence of dye leakage, as described previously (Takehana et al., 1999; Tanemura et al., 2004). The guideline for CNV scoring was as follows: no leakage (score 0); minimum leakage or a staining of tissue with no leakage (score 1); small but evident leakage less than 1/4 disc area (score 2); large evident leakage (score 3). A typical photograph of each CNV score is shown in Fig. 1. Two examiners judged the scores in a masked fashion. When the two scores given for a particular lesion did not coincide, the higher score was used for the analysis.

2.4. FITC-dextran angiogrphy

Fluorescein isothiocyanate (FITC)-dextran angiography was performed on the rats 14 days after laser induction of CNV by the method described previously (Edelman and Castro, 2000; Semkova et al., 2003), with slight modifications. The rats were deeply anesthetized and perfused with 50 mL phosphate buffered saline (PBS) with 5 mg/mL FITC-labeled dextran (MW 2×10^6; Sigma, St Louis, MO, USA) via the left ventricle through a 12-gauge cannula. The animals were sacrificed, and the eyes were enucleated and fixed in 4% paraformaldehyde for 5 h. Retinal pigment epithelium (RPE)-choroid-sclera flat mounts were obtained by hemisecting the eye and peeling the neural retina away from the eyecup. The flat mounts were laid flat onto a microscope slide with the RPE facing up. All flat mounts described here and later were examined with a fluorescence microscope (BX51; OLYMPUS, Tokyo, Japan) using FITC filters. The images of the laser lesions (= CNV area) were measured with computer-assisted image-analysis software (Lumina Vision; Mitani Corporation, Fukui, Japan).

2.5. Histopathologic studies

Histopathologic studies were performed on eyes from pitavastatin-treated rats and vehicle-treated rats at day 14 after laser induction of CNV. The rats were killed with an overdose of sodium pentobarbital. The eyes were enucleated and immersed overnight in PBS containing 2.5% glutaraldehyde and 4% paraformaldehyde. The retina-choroid-sclera were dehydrated and embedded in paraffin. Serial sections of 6-μm thickness were cut to determine the center of each lesion and stained

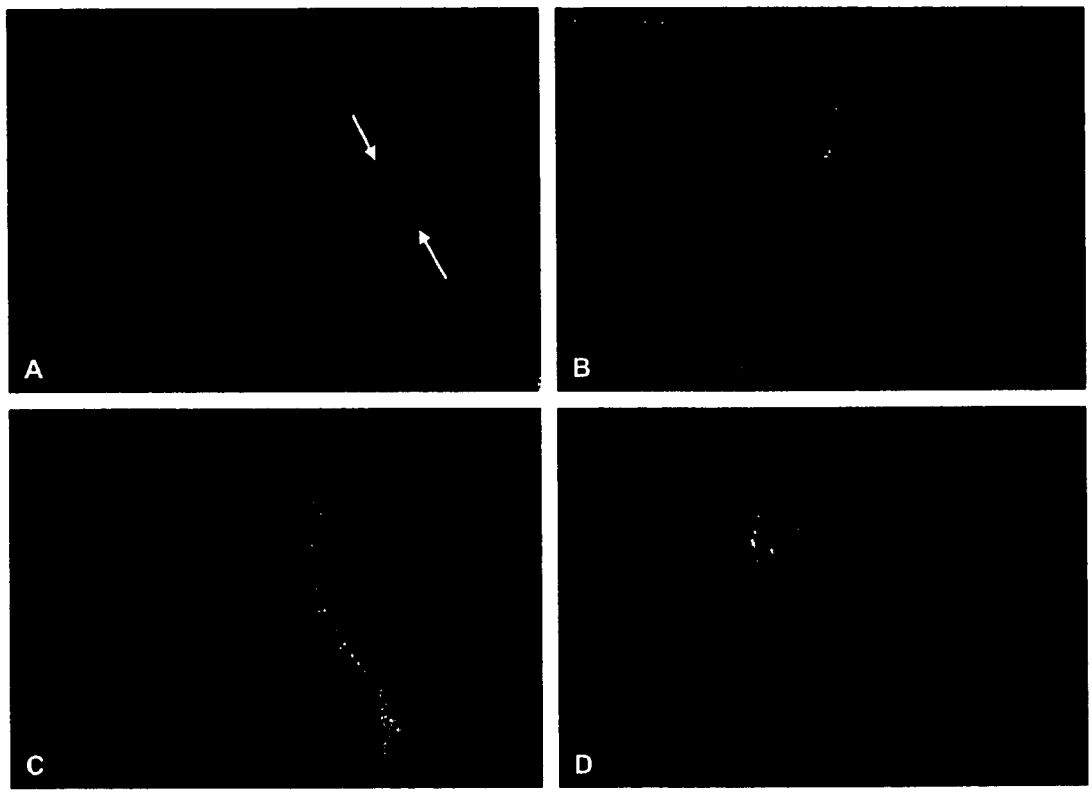

Fig. 1. Typical examples of each CNV score in the fluorescein angiogram after laser-induced CNV in rat retina. Each laser spot was scored from 0 to 3 according to the size and the presence or absence of dye leakage on the early and late phase angiogram photographs. The guideline for the CNV scoring was as follows: (A) no leakage (score 0); (B) minimum leakage or a staining of tissue with no leakage (score 1); (C) small but evident leakage less than 1/4 disc area (score 2); (D) large evident leakage (score 3).

with hematoxylin and eosin (H&E) for light microscopy. Subsequent measurements were performed by examining stained sections under a microscope (BX51; OLYMPUS, Tokyo, Japan). The maximum CNV thickness, from the bottom of the pigmented choroidal layer to the top of the neovascular membrane, was measured using the middle section of each lesion of each eye.

2.6. RT-PCR and real-time quantitative RT-PCR

Five eyes from five rats each in the vehicle-treated and pitavastatin-treated groups were obtained to evaluate the angiogenic and inflammatory mechanism in the laser-induced CNV model, including the mRNA levels of vascular endothelial growth factor (VEGF), monocyte chemoattractant protein-1 (Ccl-2; also known as MCP-1) and intercellular adhesion molecule-1 (ICAM-1). Total RNA was isolated from the retina-RPE-choroid-sclera 3 days after laser photocoagulation using the SV Total RNA Isolation System (Promega, Madison, WI, USA) according to the manufacturer's protocol. To remove genomic DNA, the total RNA preparation was treated with DNase I (Promega, Tokyo, Japan). Reverse-transcription polymerase chain reaction (RT-PCR) was performed with 10 ng of total RNA on a 9800 Fast Thermal Cycler (Applied Biosystems, Foster City, CA, USA) using the SuperScript One-Step RT-PCR with Platinum Taq (Invitrogen, Carlsbad, CA, USA) and Taqman Gene Expression assays (Applied Biosystems) to check expression of mRNAs for rat VEGF, Ccl-2, ICAM-1 and actin beta (Actb). The assay IDs are as follows: VEGF assay ID, Rn 00582395_ m1; Ccl-2 assay ID, Rn 00580555_m1; ICAM-1 Assay ID, Rn 005642227_ m1: and Actb Assay ID, Rn00667869_m1. Although these sequences of commercially available primers were undocumented, these primers were designed for spanning between exon 2 and exon 3 so that cDNA fragments were easily distinguishable from genomic fragments. Total RNA was reverse transcribed into cDNA by one cycle at 50 °C for 30 min and one cycle at 95 °C for 10 min. The cDNA was amplified for 40 cycles at 95 °C for 15 s and 60 °C for 1 min. Ten micro liter samples of these PCR products were applied to a 3% agarose gel, electrophoresed, stained with ethidium bromide, and photographed.

In addition, real-time quantitative RT-PCR was performed with 10 ng of total RNA on an ABI Prism 7000 Sequence Detection System (Applied Biosystems) using the SuperScript One-Step RT-PCR with Platinum Taq and Taqman Gene Expression assays, to quantify the mRNAs for rat VEGF, Ccl-2, ICAM-1, and Actb. Total RNA was reverse transcribed into cDNA under the same conditions as the RT-PCR. The cDNA was amplified for 50 cycles at 95 °C for 15 s and 60 °C for 1 min. Specificity of amplification products was confirmed by conducting a melting curve of the samples after each run. The threshold cycle of fluorescence units was evaluated to quantify the amount of each mRNA. VEGF, Ccl-2, and ICAM-1 mRNA levels were normalized by the Actb mRNA level.

2.7. Statistical analysis

All results are expressed as mean ± standard error (SE). The statistical significance of CNV score, CNV area, and CNV thickness was determined using an unpaired *t*-test. VEGF, Ccl-2, and ICAM-1 mRNA levels were statistically analyzed using the Mann–Whitney *U*-test. *P* values less than 0.05 were considered statistically significant.

3. Results

3.1. Fluorescein angiography

Laser spots in each vehicle-treated rat ($n = 8$) and pitavastatin-treated rat ($n = 8$) were applied and scored as follows: score 0, 1 spot, 5 spots; score 1, 14 spots, 22 spots; score 2, 19 spots, 18 spots; score 3, 11 spots, 0 spot (Fig. 2A). As shown in Fig. 2B, the mean CNV scores in pitavastatin-treated and vehicle-treated rats were 1.29 ± 0.09 and 1.89 ± 0.12, respectively. There was a statistically significant difference between these two groups ($P < 0.05$, unpaired *t*-test).

3.2. FITC-dextran angiogrphy

In the current study, FITC-dextran was used to label the blood vessel lumen, and RPE-choroid-sclera flat mounts were examined by fluorescence microscopy to follow experimental CNV 14 days after laser photocoagulation. Fig. 3A,B show fluorescent images of CNV in laser lesions in RPE-choroid-sclera flat mounts from vehicle-treated (3A) and pitavastatin-treated (3B) rats. CNV appeared as a network of broad, flat microvessels, reminiscent of choriocapillaries that spanned a circular area approximately 300 μm in diameter. The mean CNV area in pitavastatin-treated rats ($n = 11$, $29.5 \pm 2.85 \times 10^3$ μm^2) was significantly smaller than that in vehicle-treated rats ($n = 11$, $41.2 \pm 2.48 \times 10^3$ μm^2) ($P < 0.05$, unpaired *t*-test) (Fig. 3C).

3.3. Histopathologic studies

Fig. 4A,B show representative H&E-stained sections from CNV lesions 14 days after laser photocoagulation. In the laser lesions, multilayered fusiform proliferative membranes were seen in the central area of the lesion underlying the RPE to the choroid, and blood vessels with red blood cells were also seen. The thickness of CNV lesions in pitavastatin-treated rats ($n = 3$, 73.4 ± 15.4 μm) was significantly thinner than that in vehicle-treated rats ($n = 3$, 114.2 ± 8.1 μm) ($P < 0.05$, unpaired *t*-test) (Fig. 4C).

3.4. RT-PCR and real-time quantitative RT-PCR

To investigate the mechanism of the inhibitory effect of pitavastatin on experimental CNV, we performed RT-PCR and real-time quantitative RT-PCR (Fig. 5). RT-PCR revealed that VEGF, Ccl-2, and ICAM-1 mRNA levels in pitavastatin-treated rats were lower than those in vehicle-treated rats (Fig. 5A). Furthermore, real-time quantitative RT-PCR analysis revealed that VEGF, Ccl-2, and ICAM-1 mRNA levels in pitavastatin-treated rats were significantly lower than those in vehicle-treated rats ($P < 0.05$, Mann–Whitney *U*-test) (Fig. 5B–D). The expression rate of Actb almost unchanged in pitavastatin-treated rats similar to vehicle-treated rats.

4. Discussion

In the present study, we demonstrated that the therapeutic dose of pitavastatin for human hypocholesterolemia effectively suppressed experimental CNV in rats. The pitavastatin-treated group had significantly less fluorescence leakage compared with the vehicle-treated group on fluorescein angiography. The area of CNV measured by FITC-dextran angiogrphy in the pitavastatin-treated group was also significantly smaller than that in the vehicle-treated group. In addition, through histopathologic studies we showed that

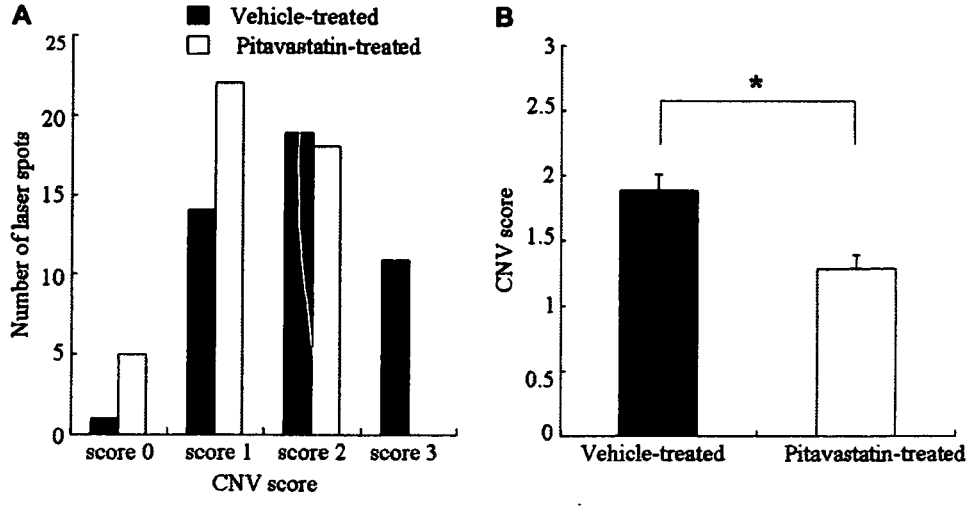

Fig. 2. Effect of pitavastatin on CNV score 14 days after laser-induced CNV in rat retina. Number of laser lesions of each 0–3 CNV scores in vehicle-treated and pitavastatin-treated rats (A). The mean CNV score in vehicle-treated and pitavastatin-treated rats (B). *, $P < 0.05$ compared with vehicle-treated.

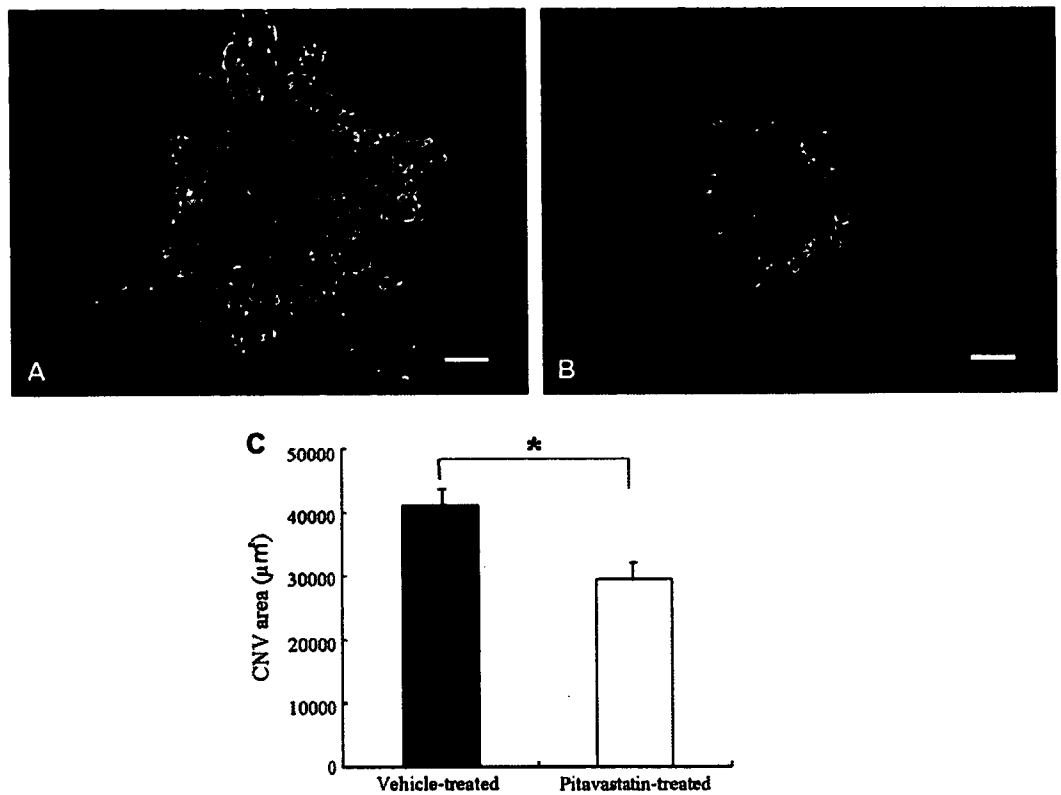

Fig. 3. Effect of pitavastatin on CNV area 14 days after laser-induced CNV in rat retina. CNV is described with green fluorescence by FITC-dextran angiography in vehicle-treated rats (A) and in pitavastatin-treated rats (B). Computer image analysis of CNV area in pitavastatin-treated rats was significantly smaller than the area in vehicle-treated rats (C). Scale bar = 100 μm (A and B). *, $P < 0.05$ compared with vehicle-treated.

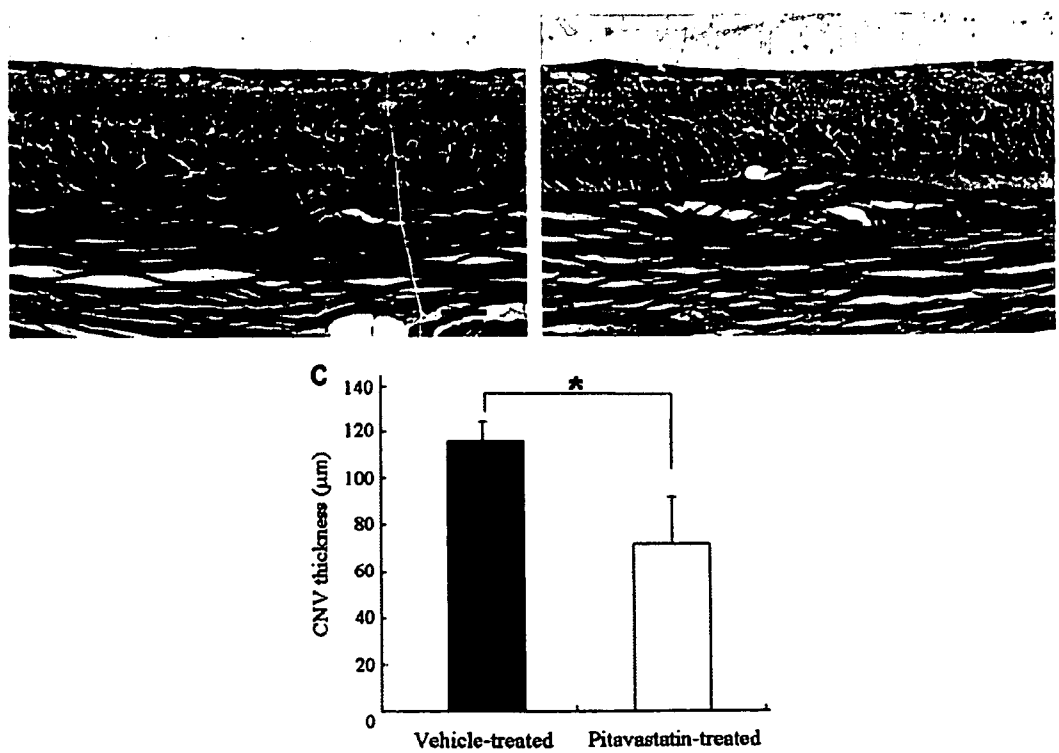

Fig. 4. Effect of pitavastatin on CNV thickness 14 days after laser-induced CNV in rat retina. Light micrographs of Hematoxylin and Eosin stained sections of the CNV lesions in vehicle-treated rats (A) and pitavastatin-treated rats (B) 14 days after laser photocoagulations. Computer image analysis of CNV thickness in pitavastatin-treated rats was significantly thinner than that in vehicle-treated rats (C). Scale bar = 100 μm (A and B). *, $P < 0.05$ compared with vehicle-treated.

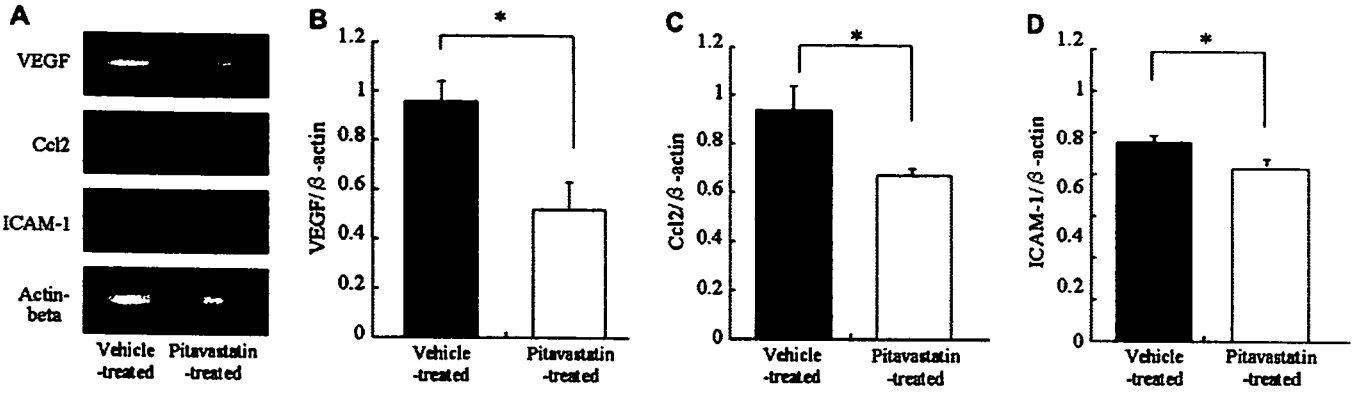

Fig. 5. Effect of pitavastatin on expression of VEGF, Ccl-2, and ICAM-1 mRNA 3 days after laser-induced CNV. RT-PCR analysis showed that VEGF, Ccl-2, and ICAM-1 mRNA expressions in pitavastatin-treated rats were lower than those in vehicle-treated rats (A). Real-time quantitative RT-PCR analysis revealed that VEGF, Ccl-2, and ICAM-1 mRNA levels in pitavastatin-treated rats were significantly decreased than those in vehicle-treated rats (B,C and D). *, $P < 0.05$ compared with vehicle-treated.

the CNV lesions in pitavastatin-treated rats were thinner than those in vehicle-treated rats. These data suggest that pitavastatin reduced the formation and development of experimental CNV. Furthermore, we present the first in vivo evidence that gene expression of VEGF, Ccl-2, and ICAM-1, which are important factors in the pathogenesis of AMD, was significantly decreased, suggesting that part of the mechanism of experimental CNV in rats is independent of the cholesterol-lowering effects of pitavastatin.

The etiology of AMD is obscure and the pathogenic pathways mediating the development of CNV are not understood. AMD and atherosclerosis have been shown to share a number of risk factors (Delcourt et al., 2001), leading to suggestions that they may have similar etiologies. The association between the use of statins and AMD has been evaluated in many clinical studies; however, the results have been contradictory (Hall et al., 2001; McCarty et al., 2001; McGwin et al., 2003; Klein et al., 2003; Wilson et al., 2004; McGwin et al., 2006). Moreover, the known pharmacodynamics of statins, such as their anti-inflammatory and anti-angiogenic effects, raises some possible mechanisms through which they may exert a protective effect in AMD.

Expression of VEGF has been demonstrated in surgically removed CNV tissues (Kvanta et al., 1996; Lopez et al., 1996) and in experimental CNV (Yi et al., 1997; Shen et al., 1998). It is well known that VEGF is the major stimulator in angiogenesis and has been shown to be correlated with the amount of inflammatory cells in CNV from AMD patients (Kvanta et al., 1996). The available in vitro data suggest that statins promote angiogenesis at lower doses, while under certain conditions some statins have the opposite effect (Urbich et al., 2002; Weis et al., 2002; Frick et al., 2003). Recently, it has been reported that therapeutic doses of pitavastatin reduced the incidence of CNV formation, but on increasing the dosage by 100-fold may exacerbate CNV leakage in experimental CNV in mice. However, retinal VEGF lysate levels did not mirror the changes in fluorescein leakage and CNV area on histological examination, suggesting a VEGF-independent mechanism for the statin effect (Zambarakji et al., 2006). In addition, we showed that therapeutic doses of pitavastatin not only reduced the incidence of CNV formation in rats but also suppressed VEGF gene expression, although we did not measure the retinal VEGF protein levels. VEGF synthesis has been shown to depend on the conditions under investigation, and the effects on VEGF were not paralleled by the angiogenic activity of endothelial cells (Frick et al., 2003).

It is well known that macrophages may play a role in the pathogenesis of AMD. Ccl-2 (also known as MCP1) is one of the most potent macrophage-recruiting molecules and is considered to be associated with the progression of CNV (Grossniklaus et al., 2002; Ambati et al., 2003). In addition, ICAM-1, which is involved in leukocyte endothelial adhesion and leukocyte migration through its receptor lymphocyte function associated antigen-1 (Mesri et al., 1994), has been proposed to be involved in the experimental CNV model (Shen et al., 1998; Sakurai et al., 2003). It has been reported that statins inhibit the expression in vitro and in vivo production of Ccl-2 (Romano et al., 2000), and leukocyte–endothelial interaction by blocking P-selectin and ICAM-1 in an ischemia-reperfusion injury model (Honjo et al., 2002). In this study, we demonstrated that pitavastatin effectively reduces gene expression of VEGF, Ccl-2, and ICAM-1 in an experimental CNV model in rats. Although we did not fully study the complex molecular mechanisms of the observed effect of pitavastatin on experimental CNV, it is possible that pitavastatin may attenuate experimental CNV development in rats through both anti-angiogenic and anti-inflammatory effects, independent of the lipid-lowering effect. Furthermore, pitavastatin (so-called vascular statin) has a high affinity for vascular endothelium. This high affinity might have had an effective on the experimental CNV.

Current treatment options for AMD are limited and to date have had little impact on the rate of blindness. Prevention of CNV formation may be important in maintaining visual function. Current preventive advice includes a suggestion for not to smoke, and possibly information regarding various supplementations; however, further preventive strategies are needed. Our data suggest that the use of pitavastatin could be helpful in

preventing CNV development in AMD patients. Furthermore, a prospective randomized controlled trial is needed to definitely address the question of statins and AMD.

References

Ambati, J., Anand, A., Fernandez, S., Sakurai, E., Lynn, B.C., Kuziel, W.A., Rollins, B.J., Ambati, B.K., 2003. An animal model of age-related macular degeneration in senescent Ccl-2- or Ccr-2-deficient mice. Nat. Med. 9, 1390–1397.

Bellosta, S., Ferri, N., Bernini, F., Paoletti, R., Corsini, A., 2000. Non-lipid-related effects of statins. Ann. Med. 32, 164–176.

Delcourt, C., Michel, F., Colvez, A., Lacroux, A., Delage, M., Vernet, M.H., 2001. Associations of cardiovascular disease and its risk factors with age-related macular degeneration: the POLA study. Ophthalmic. Epidemiol. 8, 237–249.

Edelman, J.L., Castro, M.R., 2000. Quantitative image analysis of laser-induced choroidal neovascularization in rat. Exp. Eye Res. 71, 523–533.

Fine, S.L., Berger, J.W., Maguire, M.G., Ho, A.C., 2000. Age-related macular degeneration. N. Engl. J. Med. 342, 483–492.

Frick, M., Dulak, J., Cisowski, J., Jozkowicz, A., Zwick, R., Alber, H., Dichtl, W., Schwarzacher, S.P., Pachinger, O., Weidinger, F., 2003. Statins differentially regulate vascular endothelial growth factor synthesis in endothelial and vascular smooth muscle cells. Atherosclerosis 170, 229–236.

Grossniklaus, H.E., Ling, J.X., Wallace, T.M., Dithmar, S., Lawson, D.H., Cohen, C., Elner, V.M., Elner, S.G., Sternberg Jr., P., 2002. Macrophage and retinal pigment epithelium expression of angiogenic cytokines in choroidal neovascularization. Mol. Vis. 8, 119–126.

Hall, N.F., Gale, C.R., Syddall, H., Phillips, D.I., Martyn, C.N., 2001. Risk of macular degeneration in users of statins: cross sectional study. BMJ 323, 375–376.

Hess, D.C., Fagan, S.C., 2001. Pharmacology and clinical experience with simvastatin. Expert Opin. Pharmacother. 2, 153–163.

Honjo, M., Tanihara, H., Nishijima, K., Kiryu, J., Honda, Y., Yue, B.Y., Sawamura, T., 2002. Statin inhibits leukocyte–endothelial interaction and prevents neuronal death induced by ischemia-reperfusion injury in the rat retina. Arch. Ophthalmol. 120, 1707–1713.

Jialal, I., Stein, D., Balis, D., Grundy, S.M., Adams-Huet, B., Devaraj, S., 2001. Effect of hydroxymethyl glutaryl coenzyme a reductase inhibitor therapy on high sensitive C-reactive protein levels. Circulation 103, 1933–1935.

Klaver, C.C., Assink, J.J., van Leeuwen, R., Wolfs, R.C., Vingerling, J.R., Stijnen, T., Hofman, A., de Jong, P.T., 2001. Incidence and progression rates of age-related maculopathy: the Rotterdam Study. Invest. Ophthalmol. Vis. Sci. 42, 2237–2241.

Klein, R., Klein, B.E., Tomany, S.C., Danforth, L.G., Cruickshanks, K.J., 2003. Relation of statin use to the 5-year incidence and progression of age-related maculopathy. Arch. Ophthalmol. 121, 1151–1155.

Kvanta, A., Algvere, P.V., Berglin, L., Seregard, S., 1996. Subfoveal fibrovascular membranes in age-related macular degeneration express vascular endothelial growth factor. Invest. Ophthalmol. Vis. Sci. 37, 1929–1934.

Kwak, B., Mulhaupt, F., Veillard, N., Pelli, G., Mach, F., 2001. The HMG-CoA reductase inhibitor simvastatin inhibits IFN-gamma induced MHC class II expression in human vascular endothelial cells. Swiss. Med. Wkly. 131, 41–46.

Lopez, P.F., Sippy, B.D., Lambert, H.M., Thach, A.B., Hinton, D.R., 1996. Transdifferentiated retinal pigment epithelial cells are immunoreactive for vascular endothelial growth factor in surgically excised age-related macular degeneration-related choroidal neovascular membranes. Invest. Ophthalmol. Vis. Sci. 37, 855–868.

Mahley, R.W., Huang, Y., Rall Jr., S.C., 1999. Pathogenesis of type III hyperlipoproteinemia (dysbetalipoproteinemia). Questions, quandaries, and paradoxes. J. Lipid Res. 40, 1933–1949.

McCarty, C.A., Mukesh, B.N., Fu, C.L., Mitchell, P., Wang, J.J., Taylor, H.R., 2001. Risk factors for age-related maculopathy: the Visual Impairment Project. Arch. Ophthalmol. 119, 1455–1462.

McGwin Jr., G., Modjarrad, K., Hall, T.A., Xie, A., Owsley, C., 2006. 3-hydroxy-3-methylglutaryl coenzyme a reductase inhibitors and the presence of age-related macular degeneration in the Cardiovascular Health Study. Arch. Ophthalmol. 124, 33–37.

McGwin Jr., G., Owsley, C., Curcio, C.A., Crain, R.J., 2003. The association between statin use and age related maculopathy. Br. J. Ophthalmol. 87, 1121–1125.

Mesri, M., Liversidge, J., Forrester, J.V., 1994. ICAM-1/LFA-1 interactions in T-lymphocyte activation and adhesion to cells of the blood–retina barrier in the rat. Immunology 83, 52–57.

Mitchell, P., Smith, W., Attebo, K., Wang, J.J., 1995. Prevalence of age-related maculopathy in Australia. The Blue Mountains Eye Study. Ophthalmology 102, 1450–1460.

Mitchell, P., Wang, J.J., Smith, W., Leeder, S.R., 2002. Smoking and the 5-year incidence of age-related maculopathy: the Blue Mountains Eye Study. Arch. Ophthalmol. 120, 1357–1363.

Plenge, J.K., Hernandez, T.L., Weil, K.M., Poirier, P., Grunwald, G.K., Marcovina, S.M., Eckel, R.H., 2002. Simvastatin lowers C-reactive protein within 14 days: an effect independent of low-density lipoprotein cholesterol reduction. Circulation 106, 1447–1452.

Pruefer, D., Scalia, R., Lefer, A.M., 1999. Simvastatin inhibits leukocyte–endothelial cell interactions and protects against inflammatory processes in normocholesterolemic rats. Arterioscler. Thromb. Vasc. Biol. 19, 2894–2900.

Romano, M., Diomede, L., Sironi, M., Massimiliano, L., Sottocorno, M., Polentarutti, N., Guglielmotti, A., Albani, D., Bruno, A., Fruscella, P., Salmona, M., Vecchi, A., Pinza, M., Mantovani, A., 2000. Inhibition of monocyte chemotactic protein-1 synthesis by statins. Lab. Invest. 80, 1095–1100.

Sakurai, E., Taguchi, H., Anand, A., Ambati, B.K., Gragoudas, E.S., Miller, J.W., Adamis, A.P., Ambati, J., 2003. Targeted disruption of the CD18 or ICAM-1 gene inhibits choroidal neovascularization. Invest. Ophthalmol. Vis. Sci. 44, 2743–2749.

Semkova, I., Peters, S., Welsandt, G., Janicki, H., Jordan, J., Schraermeyer, U., 2003. Investigation of laser-induced choroidal neovascularization in the rat. Invest. Ophthalmol. Vis. Sci. 44, 5349–5354.

Shen, W.Y., Yu, M.J., Barry, C.J., Constable, I.J., Rakoczy, P.E., 1998. Expression of cell adhesion molecules and vascular endothelial growth factor in experimental choroidal neovascularisation in the rat. Br. J. Ophthalmol. 82, 1063–1071.

Takehana, Y., Kurokawa, T., Kitamura, T., Tsukahara, Y., Akahane, S., Kitazawa, M., Yoshimura, N., 1999. Suppression of laser-induced choroidal neovascularization by oral tranilast in the rat. Invest. Ophthalmol. Vis. Sci. 40, 459–466.

Takemoto, M., Liao, J.K., 2001. Pleiotropic effects of 3-hydroxy-3-methylglutaryl coenzyme a reductase inhibitors. Arterioscler. Thromb. Vasc. Biol. 21, 1712–1719.

Tanemura, M., Miyamoto, N., Mandai, M., Kamizuru, H., Ooto, S., Yasukawa, T., Takahashi, M., Honda, Y., 2004. The role of estrogen and estrogen receptorbeta in choroidal neovascularization. Mol. Vis. 10, 923–932.

Urbich, C., Dernbach, E., Zeiher, A.M., Dimmeler, S., 2002. Double-edged role of statins in angiogenesis signaling. Circ. Res. 90, 737–744.

Vaughan, C.J., Gotto Jr., A.M., Basson, C.T., 2000. The evolving role of statins in the management of atherosclerosis. J. Am. Coll. Cardiol. 35, 1–10.

Wassmann, S., Faul, A., Hennen, B., Scheller, B., Bohm, M., Nickenig, G., 2003. Rapid effect of 3-hydroxy-3-methylglutaryl coenzyme a reductase inhibition on coronary endothelial function. Circ. Res. 93, e98–e103.

Weis, M., Heeschen, C., Glassford, A.J., Cooke, J.P., 2002. Statins have biphasic effects on angiogenesis. Circulation 105, 739–745.

Wilson, H.L., Schwartz, D.M., Bhatt, H.R., McCulloch, C.E., Duncan, J.L., 2004. Statin and aspirin therapy are associated with decreased rates of choroidal neovascularization among patients with age-related macular degeneration. Am. J. Ophthalmol. 137, 615–624.

Yi, X., Ogata, N., Komada, M., Yamamoto, C., Takahashi, K., Omori, K., Uyama, M., 1997. Vascular endothelial growth factor expression in choroidal neovascularization in rats. Graefes Arch. Clin. Exp. Ophthalmol. 235, 313–319.

Zambarakji, H.J., Nakazawa, T., Connolly, E., Lane, A.M., Mallemadugula, S., Kaplan, M., Michaud, N., Hafezi-Moghadam, A., Gragoudas, E.S., Miller, J.W., 2006. Dose-dependent effect of pitavastatin on VEGF and angiogenesis in a mouse model of choroidal neovascularization. Invest. Ophthalmol. Vis. Sci. 47, 2623–2631.

Zarbin, M.A., 2004. Current concepts in the pathogenesis of age-related macular degeneration. Arch. Ophthalmol. 122, 598–614.

Graefes Arch Clin Exp Ophthalmol (2008) 246:51–59
DOI 10.1007/s00417-007-0666-6

BASIC SCIENCE

Y-27632, a Rho-associated protein kinase inhibitor, attenuates neuronal cell death after transient retinal ischemia

Akira Hirata · Masaru Inatani · Yasuya Inomata · Naoko Yonemura · Takahiro Kawaji · Megumi Honjo · Hidenobu Tanihara

Received: 18 January 2007 / Revised: 19 July 2007 / Accepted: 30 July 2007 / Published online: 31 August 2007

Abstract
Purpose Transient retinal ischemia induces the death of retinal neuronal cells. Postischemic damage is associated with the infiltration of leukocytes into the neural tissue through vascular endothelia. The current study aimed to investigate whether this damage was attenuated by the inhibition of Rho/ROCK (Rho kinases) signaling, recently shown to play a critical role in the transendothelial migration of leukocytes.
Methods Y-27632, a selective inhibitor of ROCK, was injected intravitreally into rat eyes with transient retinal ischemia. Cell loss of the ganglion cell layer (GCL) and thinning of the inner plexiform layer (IPL) with and without the administration of Y-27632 were evaluated by histological anaysis, TUNEL assay and retrograde labeling of retinal ganglion cells (RGCs). To examine the attenuation of leukocyte infiltration in postischemic retinas with the administration of Y-27632, silver nitrate staining and immunohistochemistry using an anti-LCA antibody were performed.
Results Cell loss of the GCL and thinning of the IPL were significantly attenuated when 100 nmol Y-27632 was administered within three hours of the induction of ischemia. TUNEL assay and retrograde labeling of RGCs showed a decreased number of apoptotic cells and an increased number of RGCs in Y-27632-injected retinas. Moreover, silver nitrate staining and immunohistochemical analysis using an anti-LCA antibody showed that Y-27632 injection dramatically inhibited leukocyte infiltration and endothelial disarrangement.
Conclusions Our data suggest that inhibition of Rho/ROCK signaling offers neuroprotective therapy against postischemic neural damage, by regulating leukocyte infiltration in the neural tissue.

Keywords Rho · Rho kinases · Ocular hypertension · Extravasation · Cytoskeleton · Retinal ischemia

A. Hirata · M. Inatani (✉) · Y. Inomata · N. Yonemura · T. Kawaji · H. Tanihara
Department of Ophthalmology and Visual Science,
Kumamoto University Graduate School of Medical Sciences,
1-1-1 Honjo,
Kumamoto 860-8556, Japan
e-mail: inatani@fc.kuh.kumamoto-u.ac.jp

M. Honjo
Department of Ophthalmology, Kitano Hospital,
Osaka, Japan

Introduction

Retinal ischemia leads to a loss of neuronal cells in the inner retinal layers such as retinal ganglion cells (RGCs) and amacrine cells [8, 49]. Human pathological conditions associated with inner retinal neuronal cell death, including central retinal artery occlusion [13, 53, 61] and glaucoma [23, 47], have been widely studied using animal models of retinal ischemia. Such models reproducibly induce inner retinal neuronal cell apoptosis.

Neuronal cell apoptosis induced by transient retinal ischemia progresses through the reperfusion phase rather than the ischemic phase. Injury during reperfusion is caused by the infiltration of leukocytes into the neural tissue through vascular endothelia [53, 54]. During the transendothelial migration of leukocytes known as extravasation, endothelial permeability and leukocyte adhesion to endothelial cells are affected by chemokines, their receptors, adhesion molecules, and cytoskeletal components [31, 38, 51, 59]. Recently, evidence has accumulated suggesting

that leukocyte extravasation is also associated with the pathological mechanisms of retinal diseases accompanied by persistent visual disturbance, such as age-related macular degeneration [2, 48, 60] and macular edema [42, 55]. These studies show that animal models of ischemic reperfusion are powerful tools for investigating the pathological processes of retinal neuronal cell death and leukocyte extravasation.

The small GTP-binding protein, Rho, contributes to leukocyte extravasation by regulating the leukocyte cytoskeleton and tight junction of endothelial cells [39, 57]. Rho promotes myosin light chain phosphorylation by activating downstream effecters, Rho kinases (ROCKs), resulting in actomyosin-based contraction and the formation of stress fibers [1, 44]. We therefore hypothesized that the Rho/ROCK signaling pathway would play a critical role in leukocyte extravasation after transient retinal ischemia. We predicted that inactivation of Rho/ROCK signaling would contribute to the neuroprotectivity of neuronal cells in the inner retina against the reperfusion injury. Indeed, a previous study showed that Y-27632, an inhibitor of ROCKs, attenuated leukocyte recruitment following cardiac ischemic-reperfusion damage, resulting in decreased cell loss in cardiac muscle [4]. We anticipated that the inhibition of Rho/ROCK signaling could lead to a therapeutic approach for retinal diseases. To this end, we evaluated the capacity of Y-27632 to inhibit leukocyte extravasation after transient retinal ischemia and attenuate postischemic neuronal cell death.

Materials and methods

Animals

Male Sprague-Dawley rats (8–12 weeks old, 180–200 g; Kyudo, Kumamoto, Japan) were used in this study. All experiments were performed in accordance with the Statement on the Use of Animals of the Association for Research in Vision and Ophthalmology. Transient ocular hypertension was induced in the right eye of each rat, according to the method of Rosenbaum et al. [49], with slight modifications. Rats were anesthetized with a 1:1 mixture of xylazine hydrochloride (4 mg/kg; Bayer Healthcare, Tokyo, Japan) and ketamine hydrochloride (10 mg/kg; Sankyo, Tokyo, Japan). Dilation of the pupil was achieved with 0.5% tropicamide and 2.5% phenylephrine hydrochloride (Santen, Osaka, Japan). The anterior chamber of the right eye was cannulated with a 30-gauge needle and the intraocular pressure (IOP) was raised to 130 mm Hg by infusing balanced salt solution through a line attached to the needle. Completed non-perfusion was confirmed via an operating microscope (Carl Zeiss Japan, Tokyo, Japan). After 60 min of ocular hypertension, the needle was withdrawn and the IOP was normalized. The operating microscope was also used to verify reperfusion of the vessels.

Chemicals and drug administration

The dosage effects of Y-27632 (Calbiochem-Novabiochem, San Diego, CA, USA) were evaluated by injecting 1, 10, or 100 nmol Y-27632 into the vitreous, using Hamilton syringe with a 30-gauge sharpened needle (Ito, Shizuoka, Japan) aided by microscopy, 5 min before the induction of ocular hypertension. The temporal effects of Y-27632 were analyzed by injecting 100 nmol Y-27632 at 5 min, 3 h, 6 h, 12 h, 24 h, or 48 h before the induced ocular hypertension. Each dosage of Y-27632 was diluted with phosphate buffered saline (PBS) to the same final volume (1 μl) for the intravitreal injection.

Histological analysis

Histological evaluation was performed as described previously [41]. Briefly, seven days after the induction of ocular hypertension, the rats were killed by an intraperitoneal overdose injection of pentobarbital (Dainippon Seiyaku, Osaka, Japan). The eyes were enucleated and immersed in a fixative containing 2.5% glutaraldehyde and 2% paraformaldehyde (PFA) in 0.1 M phosphate buffer (pH 7.4) for 24 h at 4°C, followed by dehydration and embedding in paraffin. Transverse, 4-μm thick sections were made through the optic disc, stained with hematoxylin and eosin, and subjected to histological analysis. The degree of hypertension-induced neuronal damage in the retina was quantified by means of cell counts in the ganglion cell layer (GCL) and by measuring the thickness of the inner plexiform layer (IPL), 1.5 mm from the optic disc. Three sections for each eye were randomly selected. The cell count in GCL and the thickness of IPL were averaged in the three sections. Eight eyes were performed in each experimental condition.

Terminal deoxyribonucleotidyl transferase (TdT)-mediated fluroscein-16-dUTP nick end-labeling (TUNEL) assay

It has previously been shown in a rat model of retinal ischemia-reperfusion injury by transient elevated IOP, that TUNEL-positive cells are clearly observed in the GCL and INL 18 hours after ischemia [36]. Therefore, to evaluate the effect of Y-27632 on the attenuation of apoptosis, eyes were enucleated 18 hours after ischemia induction, and fixed in 4% PFA in PBS (pH 7.4). The TUNEL assay was performed with apoptosis detection system fluorescein (Promega, Madison, WI). The specimens were then dehydrated and embedded in paraffin and 5-μm sections

were cut. TUNEL-positive cells were counted in the GCL, and the inner nuclear layer (INL) at 1.0 to 1.5 mm from the optic disc was measured. Four eyes were evaluated for each condition.

Retrograde labeling of retinal ganglion cells

Four days after ischemia induction, retrograde labeling of retinal ganglion cells (RGCs) was performed in a manner similar to that described previously [50]. The cell count of living RGCs was performed as previously described [28, 32, 33]. Briefly, after anesthesia, rat heads were fixed in a stereotaxic apparatus. Fluoro-Gold (Fluorochrome, Englewood, CO, USA) was microinjected bilaterally into the superior colliculus. Three days after the injection, the animals were killed by an intraperitoneally injected overdose of pentobarbital. Eyes were enucleated and fixed in 4% PFA for 1 h. Retinas were divided into six segments by means of radial cuts, removed from the sclera and mounted on slides. Regions used for counting the number of Fluoro-Gold-labeled RGCs were selected from two adjacent fields in the central area (1 mm from the optic disc) from each of the six radial cuts. Thus, for each eye, 12 fields were evaluated to obtain the labeled RGC counts. Four eyes were evaluated for each condition.

Silver nitrate staining of endothelial-leukocyte interaction

Nine eyes (three eyes in each condition) were used for light microscopic studies of silver-stained endothelial cells. Six hours after ischemia induction, rats were perfused through the aorta with fixative (1% PFA and 0.5% glutaraldehyde in 0.075 M cacodylate buffer, pH 7.4) for 5 min at a pressure of 120–140 mmHg. Thereafter, the vasculature was stained with silver by perfusing five solutions in rapid succession: first, 0.9% NaCl for 2 min; second, 5% glucose for 10 s; third, 0.2% $AgNO_3$ for 7 s; fourth, 5% glucose for 10 s; and fifth, fixative for 1 min. After perfusion, the eyes were removed, cut at the equator to make eyecups, and the silver was developed by exposure to light for 15 min. After silver staining, the retinas of the eyecups were cut radially, then dehydrated in ethanol, cleared in toluene, and mounted retinal surface up.

Immunohistochemistry of infiltrating leukocytes

Twelve eyes (four eyes in each condition) were used for light microscopic studies of extravasated leukocytes. Twenty-four hours after ischemia induction, eyes were enucleated and fixed. Cryosections were blocked with 3% H_2O_2 in methanol. Sections were blocked with 10% goat serum in PBS before incubation for 1 hour with the primary antibody, a mouse anti-rat monoclonal antibody for the leukocyte common antigen (LCA)/CD45 (Serotec, Oxford, UK). Sections were then incubated for one hour with the secondary antibody, a horseradish peroxidase-conjugated goat anti-mouse IgG antibody (DAKO Japan, Kyoto, Japan). 3,3′-diaminobenzidine, tetrahydrochloride (DAB; DAKO Japan) was used as a chromogen. Cells that stained positive for LCA were counted.

Statistical analysis

Y-27632 dose effect and time course effect values were presented as means ± SE. TUNEL assay, retrograde RGC labeling and infiltrating leukocyte immunohistochemistry values were presented as means ± SD. Data were analyzed by one-way analysis of variance (ANOVA) using the post-hoc test with Fisher's protected least significant difference procedure. Differences were considered statistically significant when p-values were less than 0.05.

Results

Morphometric analysis of the neuroprotective effect of Y-27632

To investigate the protective effects of Y-27632 against retinal ischemia induced by 60 min of ocular hypertension (130 mm Hg), we performed a quantitative morphometric analysis (Fig. 1). The transient retinal ischemia was shown to have caused severe destruction of the inner retinal elements, which decreased the retinal thickness and damaged the retinal cells (Fig. 1a).

In PBS-treated eyes with ischemia, the mean cell density in the GCL was 29.8±1.8 cells/mm, which was significantly lower than the mean cell density of control retinas without ischemia (53.8±1.0 cells/mm; $p<0.0001$; Fig. 1b). Moreover, the mean IPL thickness in PBS-treated rats with ischemia (27.4±5.5 μm) was significantly reduced compared with retinas without ischemia (43.3±1.3 μm; $p<0.0001$; Fig. 1c). Compared with PBS-treated eyes with ischemia, the injection of 100 nmol Y-27632 before the induction of transient retinal ischemia resulted in significant protection against ischemic damage, as shown by the rescue of GCL mean cell number (37.7±1.1 cells/mm, $p=0.0021$; Fig. 1b) and mean IPL thickness (32.8±2.0 μm, $p=0.022$; Fig. 1c). No significant effect on GCL cell number or IPL thickness was induced by injections of either 1 nmol or 10 nmol Y-27632.

To evaluate the timing of Y-27632 administration, 100 nmol Y-27632 was given at 5 min, 3 h, 6 h, 12 h, 24 h, or 48 h before the induction of hypertension. Significant protection from ischemic damage was provided by treatment with Y-27632 5 min and 3 h prior to the induction of ischemia, compared

with control PBS-treated eyes (GCL cell count 37.7±1.1, p=0.002 and 36.0±1.5, p=0.033 respectively; Fig. 2a). Similarly, IPL thickness was significantly higher in eyes treated with Y-27632 5 min and 3 h prior to ischemia induction, compared with control PBS-treated eyes (p=0.031 and p=0.003 respectively; Fig. 2b).

Neuroprotective effects of Y-27632 evaluated by the TUNEL assay

Few TUNEL-positive cells were observed in retinas without ischemia (Fig. 3a) but, 18 hours after ischemia induction, numerous TUNEL-positive cells (mean 36.6±12.7 cells/mm) were found in the GCL and the inner nuclear layer (INL) (Fig. 3b). After treatment with 100 nmol Y-27632, the number of TUNEL-positive cells in the GCL and INL was significantly decreased (mean 20.6±1.4 cells/mm, p=0.015; Fig. 3c,d).

Analysis of the protective effects of Y-27632 by retrograde labeling of RGCs

To determine whether Y-27632 can protect from ischemia, retrograde labeling of RGCs was performed using Fluoro-Gold. The mean RGC density in eyes without ischemia was

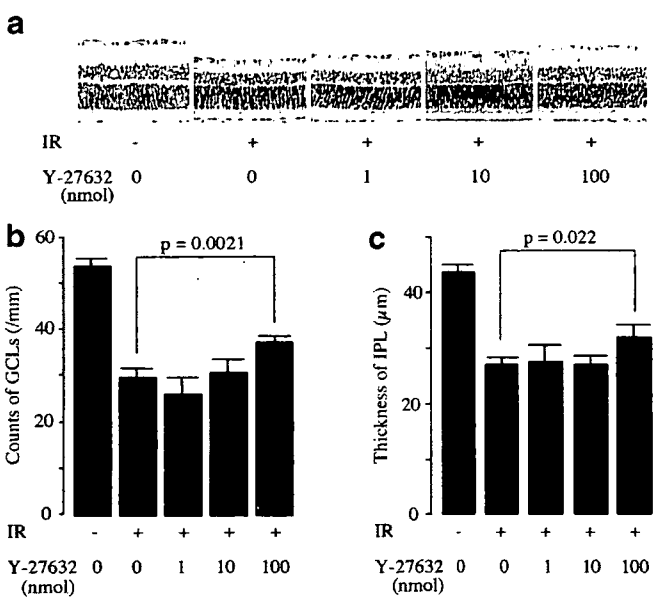

Fig. 1 Morphometric analysis of Y-27632-administered retinas after induction of transient ischemia. **a** Transverse sections stained with hematoxylin and eosin. Intravitreal injection of various concentrations of Y-27632 was performed 5 min before the induction of ocular hypertension. **b** The mean GCL cell density (/mm) at each Y-27632 concentration. **c** The mean IPL thickness (μm) at each Y-27632 concentration. Eight eyes were performed in each experimental condition. *IR*: ischemic retinal damage; +: with ischemia; −: without ischemia; *error bar*: ± SE

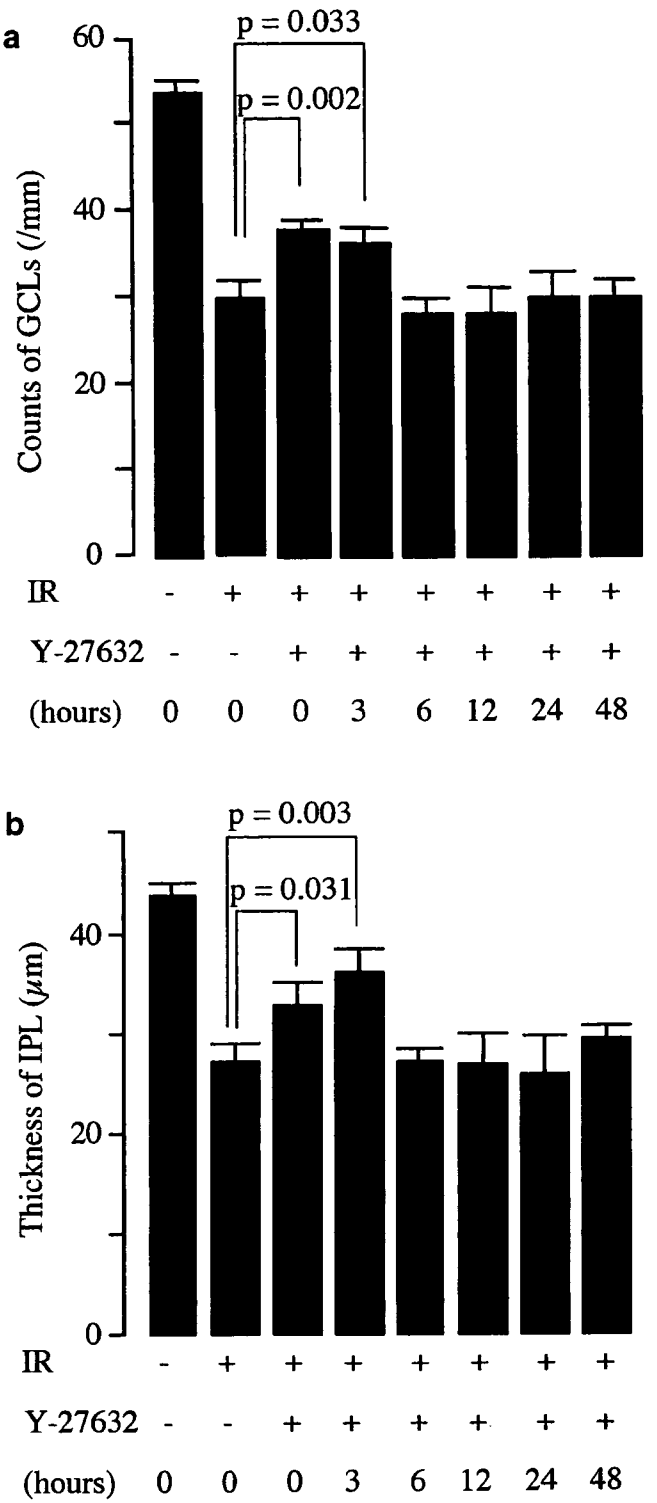

Fig. 2 Time-dependent effect of Y-27632 in retinal rescue of transient retinal ischemia. A time course of Y-27632 was evaluated by injecting 100 nmol Y-27632 at 5 min, 3 h, 6 h, 12 h, 24 h, or 48 h before induced ocular hypertension. A significant rescue of GCL cell number (**a**) and IPL thickness (**b**) was observed following administration at 5 min and 3 h prior to retinal ischemia. Eight eyes were performed in each experimental condition. *IR*: ischemic retinal damage; +: with ischemia; −: without ischemia; *error bar*: ± SE

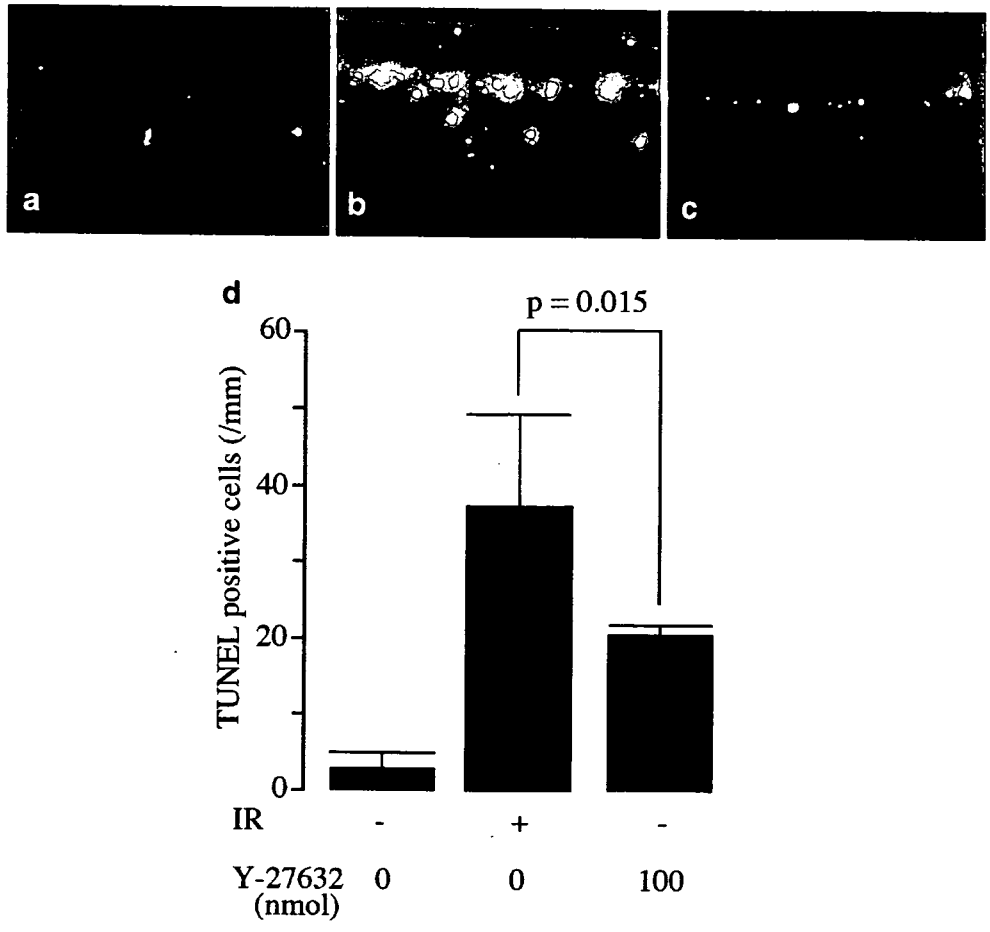

Fig. 3 Decreased number of TUNEL-positive cells in Y-27632-administered retina. Few TUNEL-positive cells were detected in retinal sections that had not undergone ischemia (**a**). Transient retinal ischemia induced TUNEL-positive cells in the GCL and INL (**b**), while administration of 100 nmol Y-27632 decreased the number of positive cells (**c**). TUNEL-positive cells were counted following each treatment (n=4) and Y-27632 shown to significantly decrease their number (**d**). *IR*: ischemic retinal damage; +: with ischemia; −: without ischemia; *error bar*: ± SE

1169.8±92.1 cells/mm^2 (Fig. 4a,d). Four days after ischemia induction, the mean density of labeled RGCs had fallen to 610.2±146.4 cells/mm^2 (Fig. 4b,d). Intravitreal injection of 100 nmol Y-27632 significantly protected RGCs against retinal ischemia, resulting in a mean RGC density of 784.7± 65.9 cells/mm^2 (p=0.015; Fig. 4c,d).

Silver nitrate staining and immunohistochemistry for infiltrating leukocytes

Endothelial cell borders were clearly stained with silver nitrate in retinal vessels without ischemia (Fig. 5a). After ischemia induction, numerous silver dots and rings, representing endothelial gaps and adherent leukocytes, respectively, were observed as previously reported [36] (Fig. 5b). Treatment with 100 nmol Y-27632 decreased the number of silver dots and rings (Fig. 5c). Few LCA-positive cells were observed in retinas without ischemia (Fig. 5d), but they increased abundantly 24 hours after ischemia induction (197.7±44.7 cells/mm; Fig. 5e,g). Treatment with 100 nmol Y-27632 decreased the number of LCA-positive cells (71.1±48.3 cells/mm; Fig. 5f,g) and the decrease was shown to be significant (p=0.007; Fig. 5g).

Discussion

The present study has demonstrated that intravitreal injection of the ROCK inhibitor Y-27632 attenuates the loss of retinal cells in the inner retinal layers after transient retinal ischemia, and that Y-27632 suppresses leukocyte recruitment and the disturbance of vascular endothelial cell alignment in the postischemic retina. Our data suggest that Y-27632 may inhibit retinal damage through regulating leukocyte infiltration in the retinal tissue. As reported previously, transient retinal ischemia induces the loss of retinal neuronal cells, especially in the inner retinal layers such as GCL and INL [46, 52]. Our ocular hypertension model, in which ischemic reperfusion in the retinal vessels has been confirmed microscopically, also drastically decreases the cell number of the GCL and the IPL thickness at 7 days after transient retinal ischemia, as described in previous reports [15, 45, 49], reflecting the destruction of the inner retinal elements.

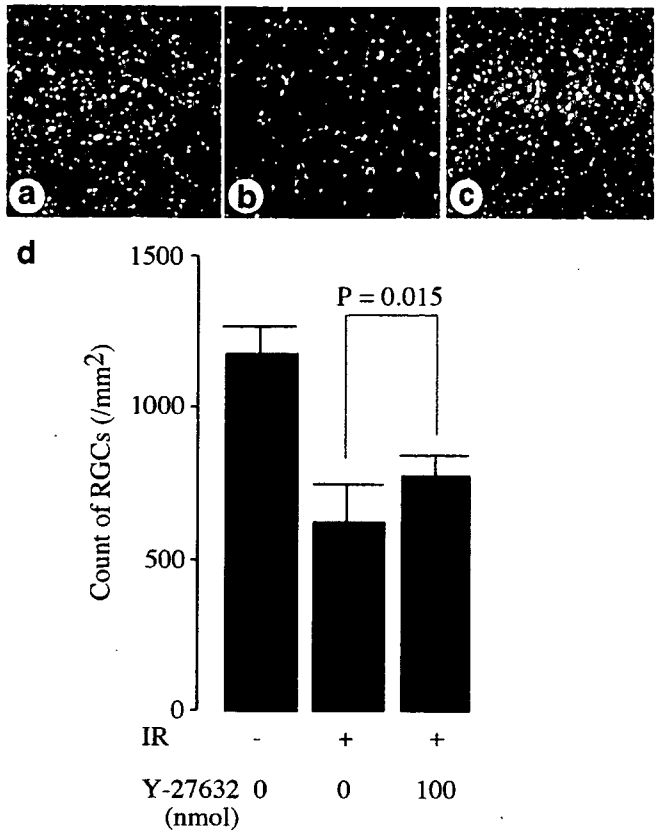

Fig. 4 Rescued RGCs in Y-27632-administered retina. Retrograde labeling of RGCs in the intact retina (**a**) by fluorescent crystal. The number of labeled RGCs decreased after transient retinal ischemia (**b**). In contrast, the number was restored by Y-27632 administration 5 min before the induction of retinal ischemia (**c**). The cell density (/mm^2) was evaluated in each condition (n=4) (**d**). +: with ischemia; −: without ischemia

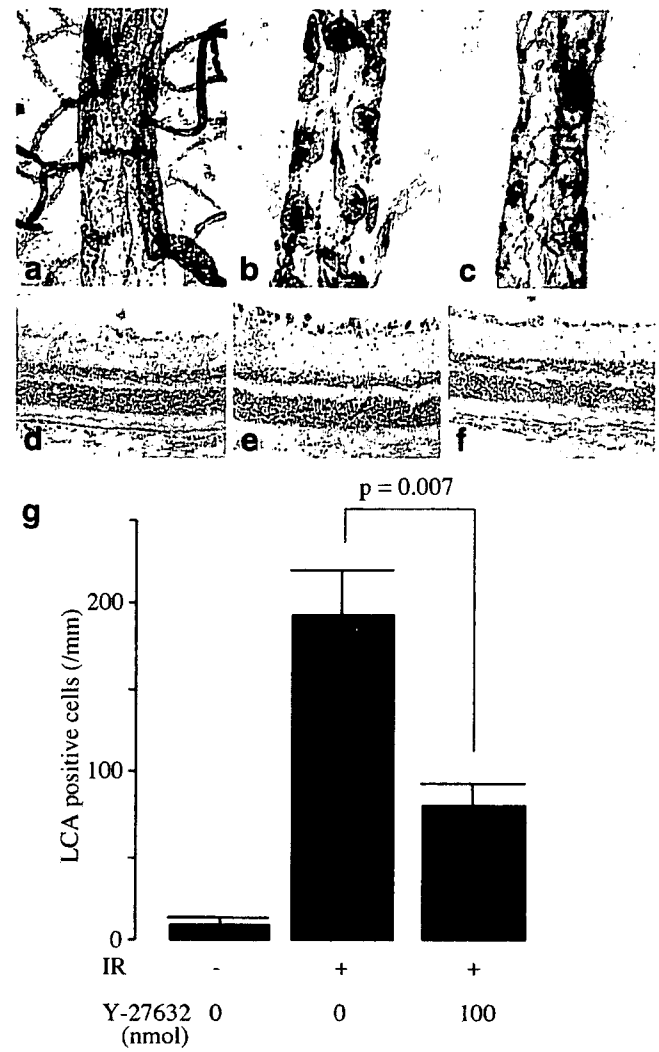

Fig. 5 Preserved endothelial gaps and diminished adherent leukocyte numbers in Y-27632-administered retinal vessels. Silver nitrate-stained endothelial cell borders in normal retinal vessels (**a**). Retinal vessels after transient ischemia demonstrated numerous silver dots and rings (**b**), which represent endothelial gaps and adherent leukocytes, respectively. Administration of Y-27632 attenuated the number of endothelial gaps and adherent leukocytes in ischemic retinal vessels (**c**). Silver nitrate-staining was performed in four eyes in each condition. LCA-positive cells (leukocytes) were few in number in normal retinal sections (**d**), while numerous immuno-positive cells were observed in the GCL after induction of transient ischemia (**e**). Administration of Y-27632 decreased the number of LCA-positive cells in the transient ischemic retina (**f**). LCA-positive cells were counted following each treatment (n=4) and 100 nmol Y-27632 was shown to significantly decrease their numbers (**g**). +: with ischemia; −: without ischemia

Recent studies have revealed that apoptosis is involved in neuronal cell death after ischemia [8, 35, 37]. Indeed, in our animal model, a significant number of TUNEL-positive cells were observed in the GCL and INL at 18 h after reperfusion, indicating apoptosis of the inner retinal cells after transient ischemia. As described previously [16, 36], TUNEL-positive cells are detected in the inner retinal layers at an early period, between 4 h and 24 h after reperfusion. These results suggest that ocular hypertension induces postischemic neuronal cell apoptosis in the GCL and INL. In contrast, when Y-27632 is administered intraviteally, cell loss and the number of apoptotic cells in the inner retina was significantly reduced. Fluoro-Gold dye is one of the most effective labeling-tracers and has been shown to label RGCs in a pair of eyes with a variance of just 4.1% [12]. Our labeling did, however, confirm that Y-27632 reduces the loss of RGCs by 28.6% after the induction of transient ischemia. Together, our data clearly demonstrate the neuroprotective effect of Y-27632 on postischemic retinal neuronal cell death.

Regarding the mechanisms of retinal damage after ischemia, leukocyte adherence to the vascular endothelium and the subsequent infiltration into postischemic tissues are reported to contribute to neuronal cell death in the postischemic area [11, 30]. Infiltrated leukocytes release oxidants and proteases, exhibiting inflammatory reactions that further increase the damage to postischemic tissue [34]. Accumulating evidence suggests that the neutralization of leukocyte

activation or the suppressed expression of leukocyte adhesion molecules on the vascular endothelial surface reduce postischemic damage and inhibit leukocyte-endothelium interaction [22, 29, 56]. The signaling pathway of Rho GTPases and their downstream effecter, ROCK, is involved in the regulation of cell motility, adhesion, and cytokinesis through the reorganization of the actin cytoskeleton and, as such, plays a critical role in leukocyte-endothelium interaction [39, 59]. It has been reported that increased expression of Rho and activation of ROCK are observed in ischemic-reperfusion tissue [4]. Moreover, a recent in vivo study demonstrated that a ROCK inhibitor reduces the infiltration of inflammatory cells into lung tissue in leukocyte-activated animal models [24]. Similarly, our present data demonstrate that injection of Y-27632 decreases the number of LCA-positive cells, indicating a decrease of recruited leukocytes in the postischemic retinal tissue. Our silver staining data also support a decrease in the number of leukocytes recruited in Y-27632-injected eyes. Although our data don't exclude the possibility that Y-27632 is neuroprotective even in the ischemic phase before reperfusion, Y-27632-induced inhibition of leukocyte activation in retinal vessels after reperfusion may attenuate neuronal cell death in the inner retinal layers.

In addition to the effects of Rho GTPases on leukocyte activation by modification of their cytoskeleton, Rho GTPase signaling pathways regulate the integrity of intercellular junctions in vascular endothelial cells, leading to accelerated trans-endothelial migration of leukocytes [17, 18, 27, 58]. Interestingly, silver staining in the postischemic retina demonstrated that the number of endothelial gaps is reduced following injection of Y-27632. This effect on the disarrangement of endothelial cells may be associated with the inhibition of Rho/ROCK signaling in endothelial cells.

The neuroprotective effect of Y-27632 is significantly observed only when the drug is administered during the early period before ischemia. We previously showed that leukocyte-endothelial cell interaction is initiated within 4 hours of reperfusion [43]. It has also been reported that Rho expression is increased 4 hours after reperfusion in an ischemic-reperfusion heart [4], indicating that Rho/ROCK signaling is activated immediately after reperfusion. It was recently reported that hydrogen peroxide, one of the neurotoxic factors secreted by leukocytes, is produced within 30 minutes of retinal reperfusion [25]. This suggests that the degenerative process involving leukocyte infiltration starts immediately after transient ischemia. Therefore, we examined whether leukocyte infiltration was attenuated by Y-27632 in the early phase after reperfusion. These previous reports are consistent with our present data and with the hypothesis that a neuroprotective effect of Y-27632 is exhibited by its attenuation of leukocyte infiltration in postischemic retinal tissues.

However, we cannot exclude the possibility that neuroprotection is exhibited through a direct inhibition of Rho/ROCK signaling within retinal neuronal cells. Interestingly, many in vitro and in vivo studies have demonstrated that Y-27632 promotes the re-growth or sprouting of injured neural fibers [7, 9, 14, 21, 40]. However, no reports have described the direct neuroprotective effects of Y-27632 in vitro. In addition, a previous study observed no direct protective effect of Y-27632 in isolated postischemic rat hearts, despite the clear demonstration of a protective effect of Y-27632 on ischemic heart muscle cells in vivo [4]. Bertrand et al. [6] reported that the intravitreal injection of the Rho antagonist C3-07 promoted the survival of RGCs as well as regeneration in the axotomized rat optic nerve. They speculated that C3-07 might have activated Müller cells that in turn influenced RGC survival. These data show that direct inhibition of Rho/ROCK signaling within neuronal cells may be associated with axon regeneration, rather than a neuroprotective effect. ROCK inhibition in leukocytes and endothelial cells may play a critical role in the neuroprotective effect of Y-27632.

We have previously reported that topical administration of Y-27632 causes IOP reduction in rabbit eyes, eliciting increased aqueous outflow via trabecular meshwork and Schlemm's canal pathway [26]. Therefore, topical administration of Y-27632 is potential for the treatment of glaucoma, in which high IOP is a major risk factor for optical damage. It has been suggested that IOP elevation results in insufficient vascular blood flow around the optic nerve head. Many studies have demonstrated ischemia at the optic nerve as a component of glaucomatous optic neuropathy [3, 5, 10, 19, 20]. Our results suggest that Rho/ROCK signaling may be a promising target for the treatment of glaucoma optic neuropathy, as its inhibition is associated not only with IOP lowering, but also with a neuroprotective effect against ischemia-induced retinal cell death.

Acknowledgements This study was supported in part by Grants-in-Aid for Scientific Research from the Ministry of Education, Science, Sports and Culture, Japan, and from the Ministry of Health and Welfare, Japan.

References

1. Amano M, Fukata Y, Kaibuchi K (2000) Regulation and functions of Rho-associated kinase. Exp Cell Res 261:44–51
2. Anderson DH, Mullins RF, Hageman GS, Johnson LV (2002) A role for local inflammation in the formation of drusen in the aging eye. Am J Ophthalmol 134:411–431
3. Anderson DR (1999) Introductory comments on blood flow autoregulation in the optic nerve head and vascular risk factors in glaucoma. Surv Ophthalmol 43:S5–S9

4. Bao W, Hu E, Tao L, Boyce R, Mirabile R, Thudium DT, Ma XL, Willette RN, Yue TL (2004) Inhibition of Rho-kinase protects the heart against ischemia/reperfusion injury. Cardiovasc Res 61:548–558
5. Bechetoille A (1996) Vascular risk factors in glaucoma. Curr Opin Ophthalmol 7:39–43
6. Bertrand J, Winton MJ, Rodriguez-Hernandez N, Campenot RB, McKerracher L (2005) Application of Rho antagonist to neuronal cell bodies promotes neurite growth in compartmented cultures and regeneration of retinal ganglion cell axons in the optic nerve of adult rats. J Neurosci 25:1113–1121
7. Borisoff JF, Chan CC, Hiebert GW, Oschipok L, Robertson GS, Zamboni R, Steeves JD, Tetzlaff W (2003) Suppression of Rho-kinase activity promotes axonal growth on inhibitory CNS substrates. Mol Cell Neurosci 22:405–416
8. Buchi ER (1992) Cell death in the rat retina after a pressure-induced ischaemia-reperfusion insult: an electron microscopic study. I. Ganglion cell layer and inner nuclear layer. Exp Eye Res 55:605–613
9. Chan CC, Khodarahmi K, Liu J, Sutherland D, Oschipok LW, Steeves JD, Tetzlaff W (2005) Dose-dependent beneficial and detrimental effects of ROCK inhibitor Y27632 on axonal sprouting and functional recovery after rat spinal cord injury. Exp Neurol 196:352–364
10. Chung HS, Harris A, Evans DW, Kagemann L, Garzozi HJ, Martin B (1999) Vascular aspects in the pathophysiology of glaucomatous optic neuropathy. Surv Ophthalmol 43:S43–S50
11. Clark WM, Lutsep HL (2001) Potential of anticytokine therapies in central nervous system ischaemia. Expert Opin Biol Ther 1:227–237
12. Danias J, Shen F, Goldblum D, Chen B, Ramos-Esteban J, Podos SM, Mittag T (2002) Cytoarchitecture of the retinal ganglion cells in the rat. Invest Ophthalmol Vis Sci 43:587–594
13. Daugeliene L, Niwa M, Hara A, Matsuno H, Yamamoto T, Kitazawa Y, Uematsu T (2000) Transient ischemic injury in the rat retina caused by thrombotic occlusion-thrombolytic reperfusion. Invest Ophthalmol Vis Sci 41:2743–2747
14. Dergham P, Ellezam B, Essagian C, Avedissian H, Lubell WD, McKerracher L (2002) Rho signaling pathway targeted to promote spinal cord repair. J Neurosci 22:6570–6577
15. Dijk F, Kamphuis W (2004) Ischemia-induced alterations of AMPA-type glutamate receptor subunit. Expression patterns in the rat retina-an immunocytochemical study. Brain Res 997:207–221
16. Dijk F, Kamphuis W (2004) An immunocytochemical study on specific amacrine cell subpopulations in the rat retina after ischemia. Brain Res 1026:205–217
17. Essler M, Amano M, Kruse HJ, Kaibuchi K, Weber PC, Aepfelbacher M (1998) Thrombin inactivates myosin light chain phosphatase via Rho and its target Rho kinase in human endothelial cells. J Biol Chem 273:21867–21874
18. Essler M, Retzer M, Bauer M, Heemskerk JW, Aepfelbacher M, Siess W (1999) Mildly oxidized low density lipoprotein induces contraction of human endothelial cells through activation of Rho/Rho kinase and inhibition of myosin light chain phosphatase. J Biol Chem 274:30361–30364
19. Flammer J (1994) The vascular concept of glaucoma. Surv Ophthalmol 38:S3–S6
20. Flammer J, Orgul S, Costa VP, Orzalesi N, Krieglstein GK, Serra LM, Renard JP, Stefansson E (2002) The impact of ocular blood flow in glaucoma. Prog Retin Eye Res 21:359–393
21. Fournier AE, Takizawa BT, Strittmatter SM (2003) Rho kinase inhibition enhances axonal regeneration in the injured CNS. J Neurosci 23:1416–1423
22. Gidday JM, Gasche YG, Copin JC, Shah AR, Perez RS, Shapiro SD, Chan PH, Park TS (2005) Leukocyte-derived matrix metalloproteinase-9 mediates blood-brain barrier breakdown and is proinflammatory after transient focal cerebral ischemia. Am J Physiol Heart Circ Physiol 289:H558–H568
23. Hara H, Ichikawa M, Oku H, Shimazawa M, Araie M (2005) Bunazosin, a selective alpha1-adrenoceptor antagonist, as an anti-glaucoma drug: effects on ocular circulation and retinal neuronal damage. Cardiovasc Drug Rev 23:43–56
24. Hashimoto T, Yamashita M, Ohata H, Momose K (2003) Lysophosphatidic acid enhances in vivo infiltration and activation of guinea pig eosinophils and neutrophils via a Rho/Rho-associated protein kinase-mediated pathway. J Pharmacol Sci 91:8–14
25. Hirooka K, Miyamoto O, Jinming P, Du Y, Itano T, Baba T, Tokuda M, Shiraga F (2006) Neuroprotective effects of D-allose against retinal ischemia-reperfusion injury. Invest Ophthalmol Vis Sci 47:1653–1657
26. Honjo M, Tanihara H, Inatani M, Kido N, Sawamura T, Yue BY, Narumiya S, Honda Y (2001) Effects of rho-associated protein kinase inhibitor Y-27632 on intraocular pressure and outflow facility. Invest Ophthalmol Vis Sci 42:137–144
27. Hordijk PL, ten Klooster JP, van der Kammen RA, Michiels F, Oomen LC, Collard JG (1997) Inhibition of invasion of epithelial cells by Tiam1-Rac signaling. Science 278:1464–1466
28. Inomata Y, Hirata A, Yonemura N, Koga T, Kido N, Tanihara H (2003) Neuroprotective effects of interleukin-6 on NMDA-induced rat retinal damage. Biochem Biophys Res Commun 302:226–232
29. Ishikawa M, Cooper D, Russell J, Salter JW, Zhang JH, Nanda A, Granger DN (2003) Molecular determinants of the prothrombogenic and inflammatory phenotype assumed by the postischemic cerebral microcirculation. Stroke 34:1777–1782
30. Ishikawa M, Zhang JH, Nanda A, Granger DN (2004) Inflammatory responses to ischemia and reperfusion in the cerebral microcirculation. Front Biosci 9:1339–1347
31. Johnson-Leger C, Aurrand-Lions M, Imhof BA (2000) The parting of the endothelium: miracle, or simply a junctional affair? J Cell Sci 113:921–933
32. Kido N, Tanihara H, Honjo M, Inatani M, Tatsuno T, Nakayama C, Honda Y (2000) Neuroprotective effects of brain-derived neurotrophic factor in eyes with NMDA-induced neuronal death. Brain Res 884:59–67
33. Kido N, Inatani M, Honjo M, Yoneda S, Hara H, Miyawaki N, Honda Y, Tanihara H (2001) Dual effects of interleukin-1beta on N-methyl-D-aspartate-induced retinal neuronal death in rat eyes. Brain Res 910:153–162
34. Kontos CD, Wei EP, Williams JI, Kontos HA, Povlishock JT (1992) Cytochemical detection of superoxide in cerebral inflammation and ischemia in vivo. Am J Physiol 263:H1234–H1242
35. Kuroiwa S, Katai N, Shibuki H, Kurokawa T, Umihira J, Nikaido T, Kametani K, Yoshimura N (1998) Expression of cell cycle-related genes in dying cells in retinal ischemic injury. Invest Ophthalmol Vis Sci 39:610–661
36. Lam TT, Abler AS, Tso MO (1999) Apoptosis and caspases after ischemia-reperfusion injury in rat retina. Invest Ophthalmol Vis Sci 40:967–975
37. Levin LA, Louhab A (1996) Apoptosis of retinal ganlion cells in anterior ischemic optic neuropathy. Arch Ophthalmol 114:488–491
38. McDonald DM (1994) Endothelial gaps and permeability of venules in rat tracheas exposed to inflammatory stimuli. Am J Physiol 266:L61–L83
39. Millán J, Ridley AJ (2005) Free in PMC Rho GTPases and leucocyte-induced endothelial remodelling. Biochem J 385:329–337
40. Monnier PP, Sierra A, Schwab JM, Henke-Fahle S, Mueller BK (2003) The Rho/ROCK pathway mediates neurite growth-inhibitory activity associated with the chondroitin sulfate proteoglycans of the CNS glial scar. Mol Cell Neurosci 22:319–330

41. Morizane C, Adachi K, Furutani I, Fujita Y, Akaike A, Kashii S, Honda Y (1997) N(omega)-nitro-L-arginine methyl ester protects retinal neurons against N-methyl-D-aspartate-induced neurotoxicity in vivo. Eur J Pharmacol 328:45–49
42. Musashi K, Kiryu J, Miyamoto K, Miyahara S, Katsuta H, Tamura H, Hirose F, Yoshimura N (2005) Thrombin inhibitor reduces leukocyte-endothelial cell interactions and vascular leakage after scatter laser photocoagulation. Invest Ophthalmol Vis Sci 46:2561–2566
43. Nishijima K, Kiryu J, Tsujikawa A, Miyamoto K, Honjo M, Tanihara H, Nonaka A, Yamashiro K, Katsuta H, Miyahara S, Honda Y, Ogura Y (2004) Platelets adhering to the vascular wall mediate postischemic leukocyte-endothelial cell interactions in retinal microcirculation. Invest Ophthalmol Vis Sci 45:977–984
44. Olson MF (2004) Contraction reaction: mechanical regulation of Rho GTPase. Trends Cell Biol 14:111–114
45. Osborne NN, Larsen AK (1996) Antigens associated with specific retinal cells are affected by ischaemia caused by raised intraocular pressure: effect of glutamate antagonists. Neurochem Int 29:263–270
46. Osborne NN, Wood JP, Melena J, Chao HM, Nash MS, Bron AJ, Chidlow G (2000) 5-Hydroxytryptamine1A agonists: potential use in glaucoma. Evidence from animal studies. Eye 14:454–463
47. Osborne NN, Chidlow G, Layton CJ, Wood JP, Casson RJ, Melena J (2004) Optic nerve and neuroprotection strategies. Eye 18:1075–1084
48. Penfold PL, Madigan MC, Gillies MC, Provis JM (2001) Immunological and aetiological aspects of macular degeneration. Prog Retin Eye Res 20:385–414
49. Rosenbaum DM, Rosenbaum PS, Gupta A, Michaelson MD, Hall DH, Kessler JA (1997) Retinal ischemia leads to apoptosis which is ameliorated by aurintricarboxylic acid. Vision Res 37:3445–3451
50. Sawada A, Neufeld AH (1999) Confirmation of the rat model of chronic, moderately elevated intraocular pressure. Exp Eye Res 69:525–531
51. Springer TA (1994) Traffic signals for lymphocyte recirculation and leukocyte emigration: the multistep paradigm. Cell 76:301–314
52. Sucher NJ, Lipton SA, Dreyer EB (1997) Molecular basis of glutamate toxicity in retinal ganglion cells. Vision Res 37:3483–3493
53. Szabo ME, Droy-Lefaix MT, Doly M, Carre C, Braquet P (1991) Ischemia and reperfusion-induced histologic changes in the rat retina. Demonstration of a free radical-mediated mechanism. Invest Ophthalmol Vis Sci 32:1471–1478
54. Szabo ME, Droy-Lefaix MT, Doly M, Braquet P (1992) Ischaemia- and reperfusion-induced Na+, K+, Ca2+ and Mg2+ shifts in rat retina: effects of two free radical scavengers, SOD and EGB 761. Exp Eye Res 55:39–45
55. Tamura H, Miyamoto K, Kiryu J, Miyahara S, Katsuta H, Hirose F, Musashi K, Yoshimura N (2005) Intravitreal injection of corticosteroid attenuates leukostasis and vascular leakage in experimental diabetic retina. Invest Ophthalmol Vis Sci 46:1440–1444
56. Tsujikawa A, Ogura Y, Hiroshiba N, Miyamoto K, Kiryu J, Tojo SJ, Miyasaka M, Honda Y (1999) Retinal ischemia-reperfusion injury attenuated by blocking of adhesion molecules of vascular endothelium. Invest Ophthalmol Vis Sci 40:1183–1190
57. Wittchen ES, van Buul JD, Burridge K, Worthylake RA (2005) Trading spaces: Rap, Rac, and Rho as architects of transendothelial migration. Curr Opin Hematol 12:14–21
58. Wojciak-Stothard B, Potempa S, Eichholtz T, Ridley AJ (2001) Rho and Rac but not Cdc42 regulate endothelial cell permeability. J Cell Sci 114:1343–1355
59. Worthylake RA, Burridge K (2001) Leukocyte transendothelial migration: orchestrating the underlying molecular machinery. Curr Opin Cell Biol 13:569–577
60. Yeh DC, Bula DV, Miller JW, Gragoudas ES, Arroyo JG (2004) Expression of leukocyte adhesion molecules in human subfoveal choroidal neovascular membranes treated with and without photodynamic therapy. Invest Ophthalmol Vis Sci 45:2368–2373
61. Zhang Y, Cho CH, Atchaneeyasakul LO, McFarland T, Appukuttan B, Stout JT (2005) Activation of the mitochondrial apoptotic pathway in a rat model of central retinal artery occlusion. Invest Ophthalmol Vis Sci 46:2133–2139

Potential Role of Rho-Associated Protein Kinase Inhibitor Y-27632 in Glaucoma Filtration Surgery

Megumi Honjo,[1] *Hidenobu Tanihara,*[2] *Takanori Kameda,*[1] *Takahiro Kawaji,*[2] *Nagahisa Yoshimura,*[1] *and Makoto Araie*[3]

Purpose. To investigate the role of Y-27632, a specific inhibitor of Rho-associated protein kinase (ROCK) in regulating human Tenon fibroblast (HTF) activities including proliferation, adhesion, contraction, migratory response, and myofibroblast transdifferentiation. Effects of Y-27632 on prevention of postoperative scar formation were also examined in a rabbit model of glaucoma filtration surgery.

Methods. After treatment of HTFs with Y-27632, cell toxicity, proliferation, migration, adhesion, and contraction were studied. The cytoskeleton and α-smooth muscle actin (α-SMA) expression were examined via immunohistochemistry. In vivo studies in Japanese white rabbits consisted of a full-thickness sclerostomy followed in the 7-day postoperative period by topical application of Y-27632. Intraocular pressure, morphologic changes in bleb features, and histology of surgical sites were evaluated.

Results. Y-27632 had no direct toxicity or significant effects on cell proliferation of HTF. The cell adhesion assay showed that Y-27632 promoted adhesiveness to both fibronectin and collagen type I. Use of Y-27632 significantly inhibited collagen gel contraction and α-SMA expression in HTFs. Y-27632 also increased HTF motility. In vivo, Y-27632 inhibited wound healing and fibroproliferation after filtration surgery and significantly improved surgical outcome compared with the vehicle. Histologic examination revealed that blebs in the Y-27632-treated group differed from those in the vehicle-treated group in that they lacked significant collagen deposition in the sclerostomy area.

Conclusions. Y-27632 had profound effects on activities of HTFs and was effective in preventing fibroproliferation and scar formation in a rabbit model of glaucoma surgery. A ROCK inhibitor may be an effective anti-scarring agent after glaucoma filtering surgery. (*Invest Ophthalmol Vis Sci.* 2007;48: 5549–5557) DOI:10.1167/iovs.07-0878

From the [1]Department of Ophthalmology and Visual Sciences, Kyoto University Graduate School of Medicine, Kyoto, Japan; the [2]Department of Ophthalmology and Visual Science, Kumamoto University Graduate School of Medical Sciences, Kumamoto, Japan; the [3]Department of Ophthalmology, Graduate School of Medicine, University of Tokyo, Tokyo, Japan.

Supported by a Grant in Aid for Scientific Research from the Japan Society for the Promotion of Science (JSPS).

Submitted for publication July 13, 2007; revised August 16, 2007; accepted October 4, 2007.

Disclosure: **M. Honjo**, None; **H. Tanihara**, None; **T. Kameda**, None; **T. Kawaji**, None; **N. Yoshimura**, None; **M. Araie**, None

The publication costs of this article were defrayed in part by page charge payment. This article must therefore be marked "*advertisement*" in accordance with 18 U.S.C. §1734 solely to indicate this fact.

Corresponding author: Megumi Honjo, Department of Ophthalmology and Visual Sciences, Kyoto University Graduate School of Medicine, 54 Kawahara-cho, Shogoin, Sakyo, 606-8507, Kyoto, Japan; m_honjo@kuhp.kyoto-u.ac.jp.

The main cause of failure of glaucoma filtration surgery is postoperative scarring in the filtering bleb. Perioperative administration of antimetabolites such as 5-fluorouracil and mitomycin C (MMC) is effective in limiting the scarring process. However, use of these antiproliferative agents is accompanied by severe side effects.[1] Fibroblasts from the subconjunctival space play a key role in the scarring process. Several agents, such as antibody against transforming growth factor (TGF)-β2,[2] alkylphosphocholines,[3] and p38 inhibitors,[4] are reportedly potential alternative antiscarring therapeutic substances, in that they can regulate activities of fibroblasts, but they are not yet available for routine clinical use.

Fibroblasts generate a contractile force, which is essential for their role in the postoperative scarring process.[5] In addition, transdifferentiation of fibroblasts into myofibroblasts is a crucial step in wound healing and scar formation,[6] which is associated with expression of α-smooth muscle actin (α-SMA).[7] Enhanced α-SMA expression indicates the presence of activated fibroblasts with increased synthesis of extracellular matrix (ECM) proteins, growth factors, and integrins.[4,8]

The Rho subfamily of small GTPases (including Rho and Rac) has critical functions in regulation of actomyosin cytoskeletal organization, cell adhesion, and cell motility.[9–12] The cytoskeleton is regarded as a primary target of growth factor action and mediates several cell responses to the ECM.[10,13,14] ROCK I, one of the putative target molecules of Rho, has been identified as a Rho effector.[15] ROCKs are important for regulating focal adhesions and stress fiber formation in cultured fibroblasts and epithelial cells.[16,17] We have reported that a specific inhibitor of ROCK I, Y-27632, causes significantly reduced intraocular pressure (IOP) in rabbits and altered cell shape and the actin cytoskeleton of cultured human trabecular meshwork (TM) cells.[18] We have also demonstrated that Y-27632 has profound effects on TM cell activities.[19] In addition, Rho has been implicated in pathologic wound healing.[20]

We hypothesize that Rho plays an important role in modulation of cytoskeletal dynamics in human Tenon fibroblasts (HTFs) and thereby influences HTF activities. Although some research has implicated TGF-β-mediated growth factors in modification of HTF activities,[4,21] the effects of ROCK inhibitors on cytoskeletal organization, proliferation, and transdifferentiation into myofibroblasts in HTFs have not been fully explored. In particular, the involvement of the Rho signaling pathways in mediating such effects in animal models is unknown. Therefore, in this study we used Y-27632 to test its ability to inhibit proliferation, migration, and contraction of HTFs without toxicity. We also investigated its effect on preventing fibroproliferation and scar formation in a rabbit model of glaucoma surgery. These results suggest that this ROCK inhibitor may effectively prevent postoperative filtration bleb failure in glaucoma surgery.

Materials and Methods

Culture of HTFs

Small Tenon biopsy specimens were obtained during standard cataract surgery after selected patients had received comprehensive informa-

tion and provided written consent for the procedure. The protocol was approved by the Institutional Review Board at Kyoto University in compliance with tenets of the Declaration of Helsinki. Primary HTFs obtained from expansion cultures of the Tenon explants were propagated in Dulbecco's modified Eagle's medium (DMEM) supplemented with 10% heat-inactivated fetal calf serum and antibiotics. Cells were maintained in the logarithmic growth phase, and cells from passages 3 to 6 were used in all experiments, which were performed at least three times with similar results.

Trypan Blue Exclusion Test

The cytotoxicity of Y-27632 was evaluated via a trypan blue exclusion test. Viable cells were counted in vitro according to a previously described method.[19,22] Briefly, 5×10^5 HTFs were plated and grown for 24 hours, then treated with or without Y-27632 (1, 10, or 100 μM) for 24 hours. After trypan blue treatment, stained, and unstained cells were counted by using a hematocytometer. The percentage of cell viability was calculated according to the following formula: % cell viability = (viable cell count/total cell count) × 100. Five independent experiments were performed.

Cell Proliferation Assay

Proliferation of cultured HTFs was measured by use of the commercially available MTT (3-(4,5-dimethyl-2-thiazyl)-2, 5-diphenyl-2*H*-tetrazolium bromide) cell proliferation kit (Nacalai Tesque, Kyoto, Japan), according to the manufacturer's instructions. Cells were plated at a density of 1×10^4 cells per well in 96-well plates and were allowed to adhere for 24 hours. After cultures were washed with phosphate-buffered saline (PBS), they were incubated with or without Y-27632 (1, 10, or 100 μM) for 72 hours and then treated with 5 mg/mL MTT for 4 hours at 37°C. The relative active number of cells was determined by an automated plate reader (Bio-Rad, Hercules, CA).

Cell Adhesion Assay

The cell adhesion assay was performed as previously described.[19,23] Wells in 96-well plates were coated overnight with 10 μg/mL fibronectin (Sigma-Aldrich-Aldrich, St. Louis, MO) or 0.5 μg/mL collagen type I (Calbiochem, San Diego, CA) at 4°C. Remaining binding sites were blocked by 0.1% bovine serum albumin (BSA) in PBS. HTFs in culture medium containing 2 mg/mL BSA with or without Y-27632 (1, 10, or 100 μM) were loaded onto coated wells at 4×10^4 cells per well. After incubation for 60 minutes, unattached cells were removed and washed with PBS. Then, 100 μL of calcein-AM solution (Calbiochem) was added to each well and incubated for 60 minutes. The relative remaining number of cells was determined by an automated plate reader (Bio-Rad).

Collagen Gel Contraction Assay

This assay was performed as previously described,[19,24,25] with minor modifications. Briefly, HTFs were trypsinized and resuspended in culture medium at a density of 2.2×10^6 cells/mL, with or without Y-27632 (1, 10, or 100 μM). Collagen type I (Nitta Gelatin, Osaka, Japan), 10 × DMEM, reconstitution buffer (Nitta Gelatin), HTF cell suspension, and water were mixed in an ice bath at a ratio of 7:1:1:1. Aliquots (0.5 mL) of the resultant mixture were added to each well of 1% BSA-coated 24-well clusters and collagen gel formation was induced. DMEM (0.5 mL), with or without Y-27632 (1, 10, or 100 μM), was then placed on top of the collagen gels. After 1 hour of incubation, gels were freed from the walls of the culture wells, and diameters of the gels were scanned into a computer and measured every 24 hours for 4 days.

Immunohistochemistry

HTFs were plated on glass coverslips, cultured overnight, and then serum starved for 24 hours. Then, 10 μM lysophospholipid acid (LPA; Sigma-Aldrich) was added for 10 minutes, after which it was incubated with Y-27632 (1, 10, or 100 μM) for 30 minutes. After this exposure, the cells were fixed in 2% paraformaldehyde-PBS for 15 minutes and then blocked in 2% BSA for 30 minutes. Coverslips were incubated with anti-vinculin antibody (Sigma-Aldrich) or α-SMA antibody (Dako Japan, Kyoto, Japan) for 30 minutes. Rhodamine-phalloidin (Invitrogen-Molecular Probes, Eugene, OR) was used to counterstain the F-actin cytoskeleton. Samples were washed with PBS and incubated with FITC-conjugated secondary antibody (Chemicon, Temecula, CA) for 30 minutes. After they were washed, the cells were mounted in antifade medium and observed via the fluorescence microscope (model IX71; Olympus, Tokyo, Japan). Immunohistochemistry with rabbit specimens used the same routine procedure.

Measurement of Cell Motility Activities

HTFs were grown to confluence in 100-mm tissue culture dishes. Three or four sites in each dish were scraped with a yellow plastic pipette tip to remove the confluent cells and create a linear line. Medium was replaced with fresh medium, with or without Y-27632 (1, 10, or 100 μM). After incubation at 37°C for 9 hours, the movement of cells into the wound area was photographed by a digital microscope camera (Olympus) and analyzed via computer software (Olympus). The shortest distance between the edges of migrated HTFs (including protrusions) from both sides was measured, as previously described.[19,26]

Animals and Sclerostomy Protocol

Twelve female Japanese White rabbits (*Pasteurella* free, each 2.0 to 2.4 kg, 12 to 14 weeks old; SRC Japan, Osaka, Japan) were used. Experiments were conducted according to guidelines of the ARVO Statement for the Use of Animals in Ophthalmic and Vision Research and approved by the Animal Use Committee at Kyoto University. All investigations involving rabbits, including surgery, IOP measurements, bleb scoring, and determination of histologic features, were conducted in a blinded manner.

Rabbits were anesthetized with an intramuscular injection of ketamine hydrochloride (5 mg/kg body weight), and xylazine hydrochloride (5 mg/kg body weight). A limbus-based flap of the conjunctiva and the Tenon capsule was made at a distance of 5 mm from the limbus in the superior nasal quadrant of the right eye. A sclerostomy was performed, and a fistula was constructed toward the anterior chamber. The conjunctiva was closed with three 8-0 polyglactin 910 sutures. After bleb formation was tested, topical Y-27632 or PBS (12 μL of eye drops of 10 mM Y-27632 or the same amount of PBS) was applied to the eye. After surgery, 1 cm of 3 mg/g ofloxacin ointment was applied to the eye. Topical Y-27632 or PBS was applied for 7 postoperative days.

Clinical Evaluation of Postoperative Y-27632 Effects in a Rabbit Model of Glaucoma Filtration Surgery

Glaucoma Filtration Surgery. Baseline observations were obtained before surgery. The IOP of the rabbit eye was measured during topical instillation of anesthetic before and after surgery by using an applanation tonometer (Tonovet; Tiolat, Helsinki, Finland). IOP was monitored daily for 7 postoperative days, with values obtained at the same time each day. Blebs were examined via a slit lamp and were graded as previously described by Perkins et al.,[27] according to a qualitative scale of 1+ to 4+, reflecting increasing bleb height and size as follows: 1+, minimal height, conjunctiva thickening, no microcysts; 2+, microcysts present; 3+, elevated bleb covering 2 to 3 clock hours of the eye; and 4+, greatly elevated bleb covering more than 4 clock hours. A score of 0 indicated no observable bleb. Bleb failure was defined as the appearance of a flat, vascularized, scarred bleb in the presence of a deep anterior chamber.

Histologic Evaluation. For this study, rabbits were killed humanely 7 days after surgery. An incision was made 90° away from the

surgical site, and the whole globe was fixed in 4% paraformaldehyde in PBS for 48 hours at 4°C and was then embedded in medium (Tissue-Tek; Sakura Finetechnical, Tokyo, Japan). Serial sections were cut through the sclerostomy site. Approximately every fifth section was stained with standard hematoxylin-eosin (HE), elastica van Gieson (EVG; for collagen), or α-SMA. The extent of fibroproliferation and scar formation in sections was evaluated in a blinded manner.

Statistical Analysis

Data are presented as the mean ± SEM. Statistical comparisons of multiple groups used one-way or two-way repeated-measures analysis of variance (ANOVA) followed by the Bonferroni/Dunn post hoc test. Comparisons of two groups used Student's *t*-test with Bonferroni correction. Differences were considered statistically significant at $P < 0.05$.

Results

Toxicology of Y-27632: Effects on HTFs

The result of the trypan blue exclusion test showed that the percentage of living HTFs was 96.4% ± 0.3% in control cultures without Y-27632 treatment. In experimental cultures treated with various concentrations of Y-27632, percentages of living cells were 96.7% ± 0.4%, 97.3% ± 0.5%, and 96.5 ± 0.4 for 1, 10, and 100 μM Y-27632, respectively. These values were not significantly different from the control value.

Cell proliferation was measured by the MTT assay. The assay is based on measuring the intracellular formazan spectrophotometrically which is facilitated by active cells. The optical absorbance of Y-27632-treated cells were 0.66 ± 0.02, 0.66 ± 0.02, and 0.67 ± 0.01 for 1, 10, and 100 μM Y-27632 respectively, while that of control cells was 0.67 ± 0.03. The MTT assay revealed no significant differences between Y-27632-treated HTFs and control samples. This inhibitor thus displayed little toxicity and had no effect on proliferative activity of HTFs.

Influence of Y-27632 on Adhesion of HTFs to the ECM

Compared with controls, greater numbers of Y-27632-treated HTFs adhered to fibronectin and collagen type I, with adhesion to both fibronectin and collagen showing a Y-27632 concentration-dependent effect (Fig. 1). Results were statistically significant for both fibronectin (at 10 μM) and collagen type I (at 100 μM).

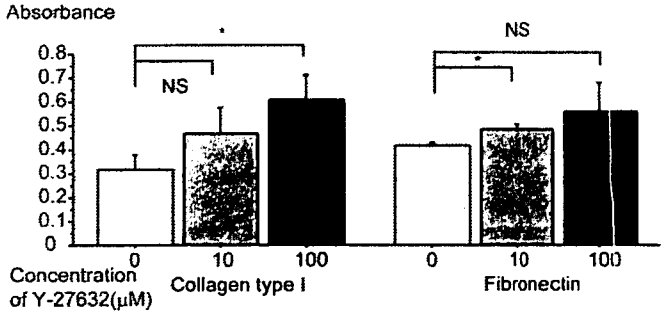

FIGURE 1. Effect of Y-27632 on adhesion of HTFs. To elucidate interactions between cultured HTFs and ECM components, adhesion of HTFs to fibronectin-coated or collagen type I–coated dishes was investigated. The cells were plated on dishes coated with fibronectin (10 μg/mL) or collagen type I (0.5 μg/mL) and were allowed to adhere in the absence or presence of 10 or 100 μM Y-27632 for 60 minutes. Adherence was measured by means of the calcein-AM assay. The relative remaining number of cells was determined based on optical absorbance of fluorescence with an emission wavelength of 520 nm measured by an automated plate reader. Data are expressed as the mean ± SEM ($n = 6$). *$P < 0.05$ versus control.

Effects of Y-27632 on the Cytoskeleton and on α-SMA Expression

In an immunohistochemical study, LPA treatment induced assembly of actin stress fibers and increased the number of focal adhesions in HTFs. Addition of Y-27632 prevented this assembly and focal adhesion expression (Figs. 2A, 2B). Addition of LPA, however, caused redistribution of focal adhesions in the cell periphery. (Fig. 2B).

HTFs were stimulated with LPA in the presence of 10 μM Y-27632 or vehicle control. Although untreated serum-starved cells showed weak α-SMA staining, LPA treatment induced assembly of α-SMA-positive stress fibers in approximately 50% of the cells, and addition of Y-27632 prevented these LPA-induced effects (Fig. 2C).

Gel Contraction Assay

Compared with controls, Y-27632 caused significant concentration-dependent inhibition of HTF-mediated collagen gel contraction in the presence of serum (Fig. 3A). At 48 hours after plating and incubation without Y-27632, the original diameter of the gels (16 mm) changed to 5.5 ± 0.2 mm ($n = 4$). However, with addition of 1, 10, or 100 μM Y-27632, collagen gel diameters at the same time point measured 4.4 ± 0.4, 1.9 ± 0.2, and 0.4 ± 0.2 mm, respectively (Fig. 3B). Experiments at 72 and 96 hours produced similar results. Results were statistically significant, and dose dependency was evident ($P < 0.001$).

HTF Cell Motility Activities

At 9 hours after the scraping, the distance between the edges of the exposed regions was 71.7% ± 4.4%, 51.2% ± 3.6%, 24.9% ± 3.0%, 7.6 ± 2.8% respectively, with Y-27632 at 0 (control), 1, 10, and 100 μM (Fig. 4). The increase in Y-27632-induced wound healing was significant and depended on concentration.

Effects of Y-27632 on Filtration Blebs

Topical instillation of Y-27632 significantly improved the results of glaucoma filtration surgery in this rabbit model and prolonged bleb survival compared with vehicle-treated control animals. Figure 5A shows the typical appearance of the blebs during the 7 postoperative days. Slit lamp examination showed that the treatment with Y-27632 was associated with elevated, diffuse blebs with mild conjunctival injection rather than the flat, scarred, vascularized blebs in the controls. In the vehicle-treated controls, vascularization in the conjunctiva was significant. Although no significant differences in anterior chamber depth or anterior chamber inflammation were observed between Y-27632-treated and control groups, postoperative IOP was significantly lower in the Y-27632-treated group (Fig. 5B). No significant postoperative changes in pupil dilation or cornea were observed in both groups. Analysis of bleb scores revealed significant differences between the Y-27632-treated and vehicle-treated control groups (Fig. 5C).

Effects of Y-27632 on Histologic Characteristics of Eyes in a Rabbit Model of Glaucoma Filtration Surgery

Surgical sites were examined 7 days after the surgery and stained with HE, EVG, or α-SMA. HE stain of vehicle-treated eyes exhibited nearly complete scarring over the sclerostomy site (Fig. 6A), including evidence of new collagen deposition in the scleral gap and bleb area, as shown by EVG stain (Fig. 6C).

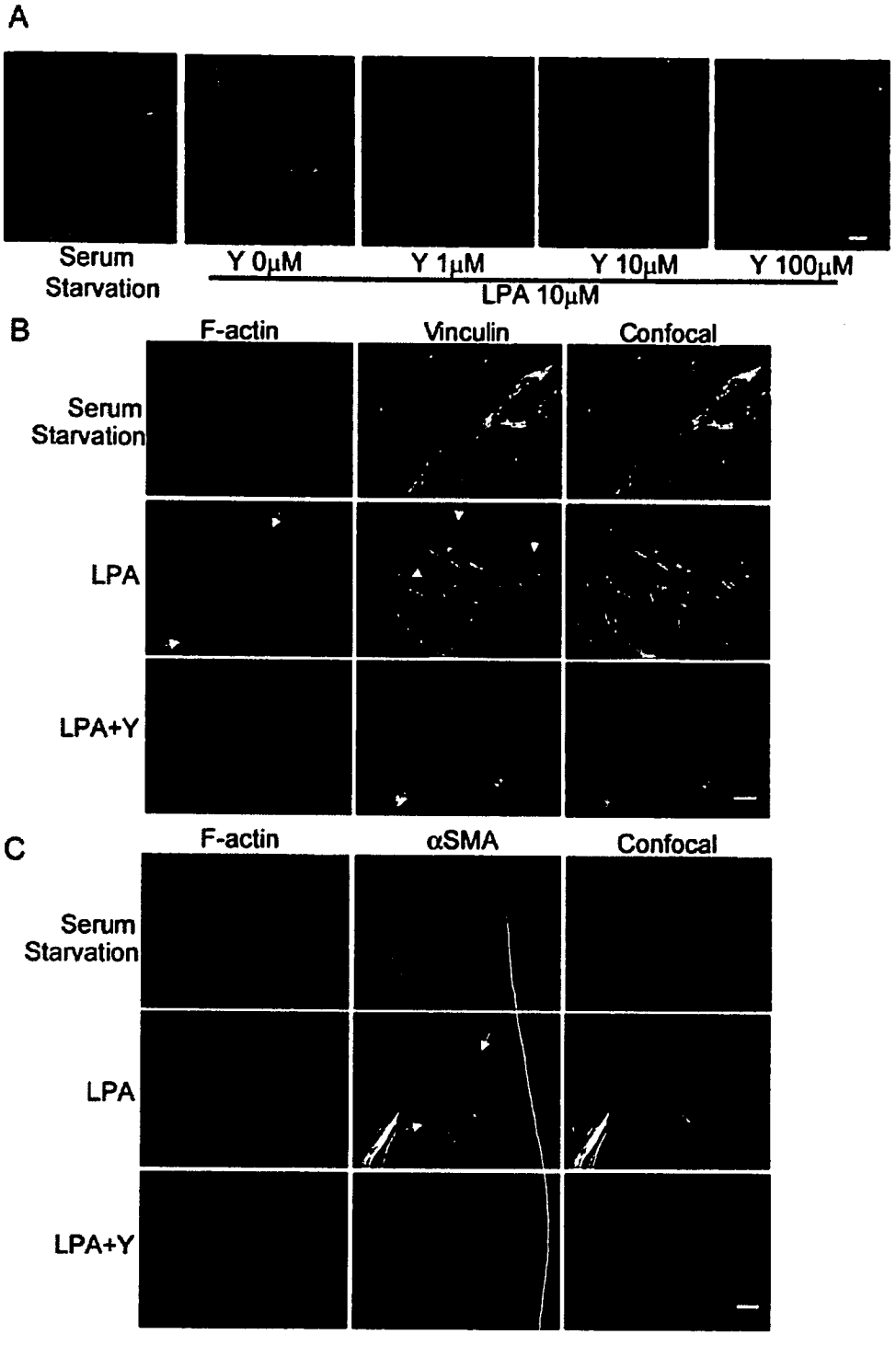

FIGURE 2. Effect of Y-27632 on the cytoskeleton and on α-SMA expression. (A) Distribution of F-actin in HTFs. Serum-starved HTFs were incubated with 10 μM LPA for 10 minutes and were then incubated without (control, 0 μM) or with 1, 10, or 100 μM Y-27632 for 30 minutes. Experiments repeated three times yielded similar results. (B) Distribution of F-actin and vinculin in HTFs. Serum-starved HTFs were stimulated with 10 μM LPA for 10 minutes and were then incubated with 10 μM Y-27632 for 30 minutes. LPA induced assembly of actin stress fibers (B, *white arrows*) and redistribution of focal adhesions in the cell periphery (B, *white arrowheads*), and Y-27632 prevented these effects. *Right*: merged images. (C) Distribution of F-actin and α-SMA in HTFs. α-SMA expression is a hallmark of myofibroblast generation and the cells' fibrogenic reaction. The cells were stimulated with LPA in the presence of 10 μM Y-27632. LPA treatment induced assembly of α-SMA-positive stress fibers (C, *white arrows*). Y-27632 prevented LPA-induced expression of α-SMA and its incorporation into actin stress fibers. *Right*: merged images. Scale bars, 50 μm.

In contrast, HE stain showed that postoperative scar formation at day 7 was significantly reduced by Y-27632 treatment (Fig. 6B). EVG stain showed that eyes treated with Y-27632 had bleb cavities of moderate size and evidence of minimal deposition of new collagen in the sclera (Fig. 6D). As judged by EVG with higher magnification, both the conjunctiva and the subconjunctival scar (Fig. 6E) and the area around the failed bleb (Fig. 6G) in the vehicle-treated group consisted of dense collagen fibers and scar tissue. In contrast, the surviving Y-27632-treated bleb showed a much looser architecture with a visible conjunctiva (Fig. 6F) and bleb formation with fewer collagen deposits (Fig. 6H). The sclerostomy area in the vehicle-treated eye consisted of densely packed collagen (Fig. 6I), whereas the site in the Y-27632-treated group differed and showed loose cell infiltration without significant collagen deposition (Fig. 6J). At the microscopic level, no significant changes in the trabecular meshwork were observed after Y-27632-treatment compared with the vehicle-treated group.

Immunohistochemical staining of blebs on postoperative day 7 demonstrated reduced expression of α-SMA after Y-27632 treatment (Fig. 6K) compared with the control (Fig. 6L).

DISCUSSION

Scarring is a major reason for failure of filtration surgery. Several studies showed that subconjunctival scarring of the

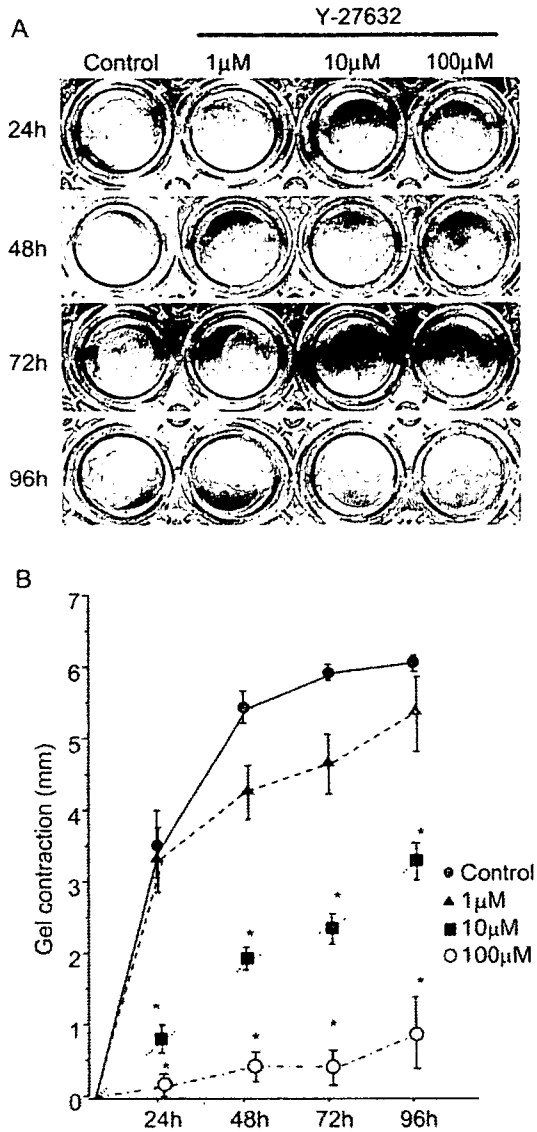

FIGURE 3. Effects of Y-27632 on HTF-mediated collagen gel contraction. (A) Collagen gels were incubated without (Control) or with Y-27632 (1, 10, or 100 μM) for up to 96 hours. (B) The extent of contraction of collagen gels mediated by HTFs was expressed as the decrease in gel diameter compared with the initial diameter. Changes in diameters of collagen gels in the absence (control) or presence of Y-27632 at 1, 10, or 100 μM were measured. Data are shown as the mean ± SEM (n =4). $P < 0.001$ versus control. Compared with the control, Y-27632 caused statistically significant, concentration-dependent inhibition of HTF-mediated collagen gel contraction ($P < 0.001$).

filtering bleb site is mainly mediated by HTF proliferation, migration, and contraction.[28-30] Fibroblasts, including HTFs,[21] are stimulated by growth factors to differentiate into myofibroblasts both in vitro[31-33] and in vivo.[34] Myofibroblasts are responsible for fibrosis via increased ECM synthesis, for granulation tissue formation, and wound contraction.[35,36]

The use of antimetabolites has been one of the most important developments in glaucoma surgery.[37,38] However, antimetabolite treatment can result in several postoperative bleb-related problems.[1,39,40] Therefore, alternative anti-scarring agents that do not cause extensive tissue damage are needed. In the present study, a specific ROCK inhibitor, Y-27632, induced profound changes in cultured HTFs without significant toxicity or inhibition of HTF proliferation. In addition, topical instillation of Y-27632 was highly effective in reducing scar tissue formation in a rabbit model of glaucoma filtration surgery.

Our in vitro results revealed that exposure to Y-27632 enhanced adhesiveness of cells to the ECM. This finding correlates well with our previous report on TM cells.[19] The actin cytoskeleton is known to interact with integrins to regulate cell shape and adhesiveness of cells to the ECM. Y-27632 reportedly promotes integrin adhesion in cultured THP-1 monocytes.[41] Our immunocytochemical investigation in the present study documented redistribution of focal adhesions in the cell periphery (Fig. 4B). This increased adhesiveness of cells to the ECM may be related to alterations in cell shape and redistribution of focal adhesions to the cell periphery.

LPA, a bioactive lipid growth factor that is present in aqueous humor, regulates various cellular events.[42] LPA, associated with activation of the Rho, induces very strong actin fibers and focal adhesions in various kinds of cells. A previous study of myofibroblasts demonstrated that LPA and serum, as well as TGF-β, could activate myofibroblast differentiation.[43,44] which is supposedly one of the most potent stimulators of HTFs.[29] After glaucoma filtration surgery, HTFs are likely to be exposed to LPA via serum and/or plasma, because the blood–aqueous humor barrier breaks down, and circulating aqueous humor bathes the wound site.[45] Y-27632 has been reported to inhibit LPA-promoted myofibroblast contraction in the collagen lattice model, which suggests that contraction depends on activation of the Rho.[46-48] In the present study, we investigated LPA-induced α-SMA expression in HTFs to analyze the direct role of the Rho signaling pathway in these cells. Treatment with Y-27632 reduced LPA-induced α-SMA expression in HTFs, which suggests that Y-27632 functions as a potent antiscarring agent via inhibition of transdifferentiation of HTFs into myofibroblasts.

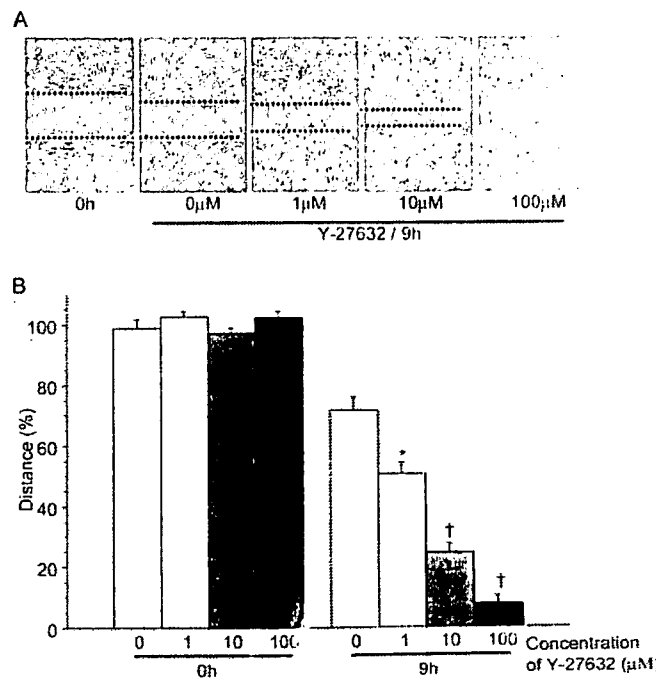

FIGURE 4. Effects of Y-27632 on cell motility activities of HTFs. (A) Confluent cultures were scraped with a yellow pipette tip to create a cell-free linear wound. Medium was replaced with fresh medium without (control) or with Y-27632 (1, 10, or 100 μM). After 9 hours, migration of cells into the wound area was photographed. *Dotted lines*: edges of the migrated cells. (B) Distances between edges of migrated cells were measured and are shown as the mean ± SEM (n = 6); the distance before treatment was set at 100%. *$P < 0.05$, †$P <$ 0.001 versus control.